Multicast scheduling for streaming video in single frequency networks

Hossein Barzegar

ROYAL INSTITUTE
OF TECHNOLOGY

Master's Degree Project

Stockholm, Sweden May 2011

Abstract

With development in wireless mobile communication and evolution to high capacity system like LTE, multimedia streaming over wireless channel becomes an interesting topic both in field of research and application. The bottleneck of this issue is limited available resources in the systems; therefore it is important how the system is allocating its resources to deliver different streams to the subscribers.

Transmitting data content in a mobile cell can be either uni-cast or multicast transmission. In multicasting type, data content is delivered simultaneously to all users within a group who already subscribed for that special stream. In both transmissions, an algorithm called scheduler decided which multicast group or user should be scheduled and receives the data content. Moreover the scheduler is responsible to dynamically change the transmission rate according to use-end's channel condition.

In this Master's thesis, we analyze multicast scheduling algorithms for delivering multilayer and single-layer streams to the user-end in LTE-MBSFN network. We use three scheduler algorithms, Max-Sum, Max-Prod, RRB-Max_Sum, to set up the simulation system. We evaluate the performance of algorithms on MBSFN and single cell multicast transmission, as well as the impact of using single-layer and multilayer streams.

Comparing single cell-multicast transmission and MBSFN scenario, our simulation shows that the quality of received streams is not degraded when the cell traffic load is small on both network structures. On high cell load occasion transmitting the single layer stream in MBSFN, results in low quality of service. The streaming can be offline when the scheduler has access to the data as much as it wants (i.e. saved on the hard disk) or real-time when data contents are stored on size limited buffer. We show that sending a small data bust is not an efficient way of multicasting on MBSFN and wastes the resources. Therefore in this Master thesis, we propose a Multi-group-Max_Sum algorithm that aggregates the small packet together and forms a bigger packet to efficiently use the frequency resources. The system will approach its ideal performance (offline streaming) when using a Multi-group-Max_Sum scheduler. After specific length, the buffer size doesn't have impact on the scheduler performance.

Acknowledgment

Hereby I would like to show my sincere regards and appreciation to Dr. György Dán who supervised me during this master thesis and patiently and supportively assisted me from step A to step Z.

Table of Contents

List of Figures

List of Tables

1 Introduction

1.1 Literature studies

High Capacity of LTE with peak rate of 340 Mb/s in 20MHZ bandwidth [44], nominate LTE as one of best candidate for mobile TV and multimedia services on the current cellular network. As long as the number of user is low, the usual fashion of Point to Point can efficiently deliver a stream with unit-cast transmission [44].On the other hand, P-to-P style fails dramatically on quality of service when there is large amount of users in high cell traffic load.

A multicast/broadcast technology has already being introduced by 3GPP to overcome the bottleneck of unit cast transmission [44, 46, 47]. By migration from UMTS to LTE and E-MBMS, operators have the opportunity to deliver multimedia stream and mobile video when lot of users should be served [48]. MBMS offer two solutions: SC-PtM and MBSFN [49], In Single cell transmission, all the user's favorite stream multicasts within one cell and are delivered with an intra-cell broadcast/multicast transmission .Disadvantages of this solution is great interference coming from neighboring cells which result in lower SINR. On the other hand, in MBSFN all the base stations are synchronized together and depending on geographical division, all the base station within the SFN area send the same data content *simultaneously*. In the MBSFN, users always have higher SINR and therefore can receive higher throughput. It is so well probable that some users suffer from low average throughput either due to be in deep fading area or lack of enough resources on the network. Lower throughput introduce higher packet loss and higher packet loss results in lower quality of picture. One solution to combat this situation is using scalable video coding streams. SVC-Stream contains a basic layer with low bit rate coding and two or more enhanced layers. When the user is on favorite channel condition, it can receive all layers while the low SINR users may only receive basic layer. On the high cell load, in order to keep the fairness on sharing resources among the users, base station can drop the enhancement layers packets and only delivers the basic layer packets to the subscriber [53].

No matter either in Single cell multicast or MBSFN, a challenging task is which multicast group should be selected and what would be transmission modulation and coding rate per TTI [43]. The target of multicasting is to minimize resource allocation. A resource can be frequency subcarrier, a channel time slot or orthogonal code so it is important to know how the resources are shared among the subscribers. The scheduler (an algorithm that shares the resources) based on a subscriber's status, takes decision on how much and when the resources should be allocated. The subscriber's status can be summarized according to their average throughput or signal to noise ratio (SNR) or any other utility function. Moreover the subscriber status may change due to channel condition therefore the scheduler should dynamically adapt the resource allocation

scheme. Authors in [51] has introduced two proportional fairness scheduling algorithm. These schedulers receive reported throughput from the end-user and dynamically change the resources allocation accordingly.

Despite selection process of the multicast group, another important task of scheduler is to decide what would be the transmission rate. It so obvious that the subscriber with low received power cannot be scheduled with high transmission rate, so one can say one possible solution for rate selection is that the scheduler should always adapt to the transmission rate to the weakest user.
Authors in [43] have offered 4 method of transmission rate selection based on the spectral efficiency. The MBSN condition for transmission rate is that the user on the edge should have 1 bit/HZ spectral efficiency [42]. The proposal algorithm in [43] is developed in such a way to guarantee these criteria for all subscribers.

In the system with OFDMA modulation, i.e LTE, the scheduling has two dimensions, time domain and frequency domain [55]. While in time domain, the scheduler decide for which users should receive the data content, the frequency scheduling algorithm allocate the frequency resources to each user. Due to multipath fading, the mobile wireless channel is frequency selective .based on user's transmission channel frequency response, some part of spectrum greatly is degraded by channel. If the scheduler allocates the user's frequency resources on those areas, users suffer from low SINR. Moreover frequency resources are also limited, so again the term of fairness can be used during frequency resource scheduling. There have been lots of studies on frequency resource allocation algorithms for LTE [55, 56,57]. In this Master thesis, perfect channel compensation is assumed on the frequency domain so there is no priority among the frequency resource for a user. The Frequency scheduling allocates the frequency resources to a user regardless of its position on the spectrum.

Some of scheduling algorithms are objective function as they maximize an objective like user utility function or average throughput [51] and they are mainly evaluated on how fairly can distribute resources to multicast groups' users. For delivering a multilayer stream to the multicast group' users, Authors in [22] has proposed two multicast proportional fair scheduling algorithms ,Max-Prod and Max-Sum that select transmission modulation and coding , video layer and multicast group that product and sum of users utility function in the UMTS-MBMS Network are maximized respectively.
Same as [22], there have been some other researches that focus on multimedia multicasting. In [58] authors have shown the same research method on multimedia broadcasting but in LTE-MBMS. They have defined a distortion model for multilayer streams and a wireless system model. Their objective is to minimize distortion of delivered stream and at the same time the number of ALL-FEC bytes that are sent to protect basic layer from corruption.

All the scheduling algorithms are on the second layer, but a system model is required to act as physical layer to deliver transmitted data to the users. In this master thesis LTE and MBSFN-LTE are chosen for mobile wireless network technology. In [58] authors have simulated the physical layer of LTE technology. Moreover in [12] the physical layer of MBSFN network is deeply studied and spectral performance of MBSFN is presented.

1.2 Motivation

This master thesis is based on work already carried out on paper [22]. However instead of multicasting over UMTS network, the multicasting of multi layer stream over LTE and MBSFN network is investigated. Migrating from UMTS to LTE introduces new challenges like resource allocation on frequency domain. Through our researches and simulation, we try to give answer for the following queries:

- What is effect of high SINR as achieved gain of MBSFN in multimedia multicasting?
- Compare the behavior of known scheduling algorithm on [22] over LTE and MBSFN network.
- It is interesting to see what the effect of real-time streaming and offline streaming is.

1.3 Methodology

To reach to the motivation targets, LTE wireless mobile network is simulated. The MBSFN/LTE coverage area is modeled as cellular network as Hexagonal topology with eNodeB on the center of each cell. Each cell is surrounded by six neighboring cell around (tier). The numbers of tiers are an input parameter that should be optimized .It is assumed an Omni directional antenna exists for each site. The transmission mode can be MBSFN when all the eNodeB transmit the same data content simultaneously or just multicasting on the central cell. Each multicast group has random user number. The users are distributed uniformly around the central cell. During simulation, subscribers are moving inside the cell according to mobility scenario.

The multilayer stream distortion model is taken from [22] and initially to each multicast group one stream is assigned. The sum of coding rate of all multicast group is called ***cell traffic load.***

In each simulation run, a multicast scheduler is examined and selected to work on the MAC layer. The number of multicast group is an input parameter to the simulation scenario therefore in order to examine the performance of a scheduler in different cell traffic load; six different cell traffic loads is carried out per simulation run. The simulation last for 10 seconds (10000 TTI).

In each simulation run with specific cell traffic load, based on subscriber's utility gain, the scheduler decides which multicast group and what layer should be scheduled. Transmission rate is decided based on SINR. The subscribers are informed about the scheduler decision through control channel. Then data content is pushed down to downlink physical layer and OFDM symbol is transmitted through wireless channel. The channel is model as TU6-Uranban. The subscriber calculated the SINR and the packet with lower SINR than specific threshold for scheduled MCS are dropped .then the subscribers updates their average through, packet loss rate and user utility accordingly. The achieved gain of each video layer over the current average throughput is calculated.

It is assumed the scheduler keep the same calculation values of throughput and user utility because scheduler already knows if the packet was delivered error free to the subscriber or not. In addition, the scheduler traces the average throughput of each subscriber after each scheduling

time. The achieved gain over average throughput of each layer lets the scheduler decide what the optimum decision is in next time slot.

1.4 Thesis Report Structure

This master thesis report is organized as follow: chapter two briefly give a background about the required theory of this report, it introduces E-UTRAN structure and its network element plus MBSFN network elements, it continues with wireless channel model and finally it ends up with brief description of multilayer and scalable video coding stream and distortion model of test stream in simulation .Chapter three deals with the details of system model and network parameters. The scheduling algorithms prototypes are discussed on chapter four and simulation methodologies are reviewed on the chapter five. The simulation results are shown and analyzed on chapter six and the report is end up with conclusion and future work on chapter seven and eight respectively.

2 Background

2.1 Introduction

To understand the system model and simulation process, one should understand the following topic:

1) E-UTRAN network architecture.
2) Mobile channel and propagation model.
3) Scalable video coding and Multilayer stream.

The following section introduced the above topic.

2.2 E-UTRAN Network Architecture

Figure2-1 illustrates the overall architecture and network elements of E-UTRAN (evolved-universal Terrestrial Radio Access Network) Network. LTE (Long Term Evolution) is an All-IP network structure, which is the evolved version of the 3GPP-UMTS standard. The LTE network has evolved toward a Packet Switch application with no circuit switch elements [31]. However, voice traffic is still welcome through IP Multimedia Systems (IMS) by means of VOIP.

Using MIMO 4x4, 64QAM high modulation scheme, and OFDMA technology results in a high capacity and spectral efficiency that lets the users benefit from higher throughput. The favorite throughput for LTE lets users enjoy at least 100 Mb/s download throughputs and 50 Mb/s upload throughput [27]. Such high throughput demands low latency and less packet delivery delay. Therefore, E-UTRAN offers a seamless end-to-end IP accession from user-end to Packet Data Network (PDN). To realize this goal, the number of elements involved in packet delivery enshorted in E-UTRAN structure so the base station is directly connected to the Core Network. This is contradicts the UMTS network in which the base station connects to the Core Network via Radio Network Controller, RNC. The Core Network of E-UTRAN is always referred as Evolved Packet Core (EPC), and the base station is called Evolved NodeB, eNodeB. Since eNodeB is substituted element for RNC in 3GPP release 8 and after, it takes all responsibilities of Radio Resource management, mapping channel transport to physical channels, power control, mobility management, and so on. The E-UTRAN system consists of four parts that interconnect via standard interfaces that allow different network elements to belong to different vendors:

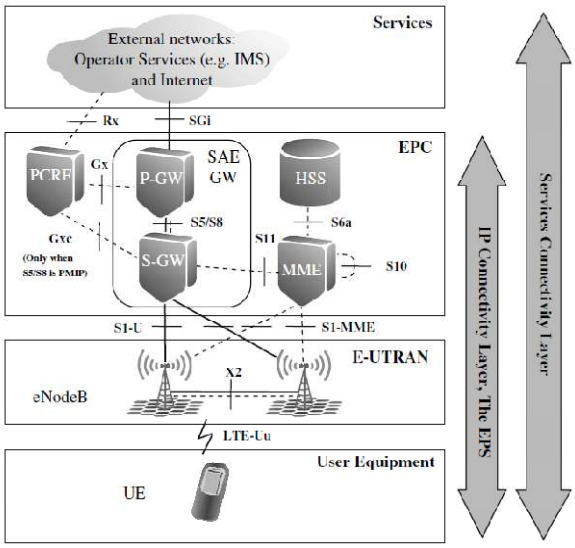

Figure 2-1 : E-UTRAN System Architecture [27]

- User Terminal.
- E-UTRAN or Radio Access Part.
- Core Network (EPC)
- Service Area

The S1 interface control and user planes terminate in different EPC network elements. The Mobility Management Entity (MEE) processes the control plane while the user plane is forwarded to Serving Gateways. Serving Gateways and Packet Gateways are referred as System Evolved Architecture, or SAE.

PCRF apply policy and charging control to any kind of 3GPP IP-CAN and any non-3GPP accesses. It also involves service data flow reports [33]. 3GPP-IP-CAN refers to any IPV4/IPV6 session initiated by user-end to connect to PDN within LTE Network or access to other RAT (Radio Access Technology) Packet Gateway. PCRF (Policy and Charging Rules Function) elements can discard any packet or any IP-CAN session initiation that has rules predefined by operators [34]. In the service connectivity layer, the flow may flow through different bearers. This IP-CAN bearer contains different data types. One consists of VOIP data, while the others may contain video conference packets or internet surfing data. The IP-CAN bearer's specification differs, depending on the type of data they bear. The EPC must provide Qos for IP service conviviality between user-end and PDN elements. The specification of each IP-CAN bearer—like its bandwidth, delays, and bit error rate—is designated to an IP bearer by PCRF. The rest of the section briefly addresses the different element rules and specifications.

2.2.1.1 User Equipment

UE is a modem used to send and receive the data through air channels. The current LTE dongle can sometimes support other radio technologies like 2G and 3G. When the LTE network coverage is poor, if Data Card and Network operators permit inter-RAT handover, LTE dongle can automatically switch to the other Radio type. There is a separate module from the rest of the UE, which is often called the Terminal Equipment. In the terminal equipment, USIM is an application that identifies and authenticates the user and derives security keys in order to protect the radio transmission [27].

2.2.1.2 E-UTRAN (eNodeB)

In the Radio access part, since there is no centralized control over base stations, the E-UTRAN is called a flat structure. eNodeB has rule of layer 2 bridge between user-end and EPC [27] to act as an access point, receiving the packets through the air channel, forwarding them to the Core Network, and vice versa.

The eNodeB is interconnected to Core Network via S1 interface. S1-U connects the eNodeB to S-GW while the S1 control plane terminates on MME. The eNodeBs on the E-UTRAN network can communicate through the X2 interface. This interface is implemented when users travels around the coverage area and need handover between two eNodeBs. Some function of eNodeB are :

- **Radio Resource Management:** The main responsibility of eNodeB is Radio Resource Management (RRM), which includes control over radio bearer, admission and initiation of new calls, paging the users, Dynamic Resource allocation on uplink and downlink, power control management, and implementation and monitoring the designated Qos of IP transport bearer.
- **IP Header Compression/Decompression:** To utilize the radio air channel interface, the eNodeb removes some IP header. This is especially useful for small IP packets. It is also advantageous when repetitive data is sent through IP headers.
- **Security:** To secure communication through the air, users' data are encrypted.
- **Mobility Management**: By periodically asking the UE to report its received signal power measurement, the eNodeB decides whether or not to initiate the handover process to neighboring

2.2.1.3 PDN(P-GW)

P-GW is responsible for allocating the IP address to the Terminal, serving the Packet access server to the internet and inserting the data packet to the IP transport bearer. It follows the predefined Qos performance enforcement rules by PCRF. It also serves the Gateway through the other 3GPP radio technologies like the Wimax, GPRS and UMTS.

2.2.1.4 S-GW

All user IP packets are transferred through the S-GW to P-GW, and it is the termination point for S1-U interface. It is also responsible to buffer the data of IP bearer while UE is in Idle Mode and MEE is paging the user. In addition, S-GW reports some data volume usage for charging policy to PCRF.

2.2.1.5 MME

The MME processes the control plane data and handles bidirectional protocol messages toward user-end, which is called Non Access Stratum Protocol. When a user is registered on the network (asks for call session initiation), MME is responsible for Authentication and Security implementation [27]. It receives the Authentication vector from HSS and compares with the one received from UE. The UE session is granted if the result is the same [34]. Attachment and de-

attachment of user-end to the core network and releasing the transport bearer are managed by MME. MME is also involved during any handover between eNodeBs, and it handles the signaling between eNodeBs. When a packet arrives to P-GW and user is in idle mode, The S-GW initiates a paging request, and MME pages the user.

2.2.2 E-UTRAN MBMS

Delivering mobile multimedia service to a large group of users requires a huge transmission resources. Transmission types can either be unitcast (point-to-point) or broadcast, which is a point-to-Multipoint data delivery. Multicast transmission is a form of broadcast p-t-m data delivery that applies only to a group of users who already subscribe for a special service, such as a TV-channel.

Broadcasting multimedia content over a single and shared resource to a group of users was already proposed in UMTS [42]. Multicast Broadcast Multimedia service, MBMS, was introduced in the release 6, and reached for a spectrum efficiency of 1 bps/Hz in the cell edge in an urban or suburban environment. This is equivalent supporting of at least 16 Mobile TV channels at around 300 kbps per channel in a 5 MHz bandwidth [42]. A challenging task of Multicast or Broadcast transmission is selecting transmission rate. In multicasting, the usual transmission rate is adapted to the lowest user's SINR.
In the LTE, an enhanced MBMS feature was proposed on release 9 [41]. Also, with OFDM as modulation technology, a new feature called the Multimedia Broadcasting Single Frequency Network or MBSFN is introduced. In the MBSFN, all the eNodeBs within a geographical area, called MBSFN area or Service area, simultaneously transmit the same data. The MBSFN greatly enhances SINR, therefore resulting in better spectral efficiency and higher throughput.
To overcome the problem of ISI, a longer cyclic prefix length is used in MBSFN frame. In addition, the reference signal pattern is changed in the MBSFN sub-frame. [27]

MBSFN requires synchronization among the all eNodeBs [42]. GPS may apply as a reference network clock source for eNodeB synchronization. Moreover, the synchronization is needed for data content, too. Synchronized content means all eNodeBs are using the same modulation rate, coding rate, and aligned resource block to prevent interference from other resource blocks containing non-MBSFN data.

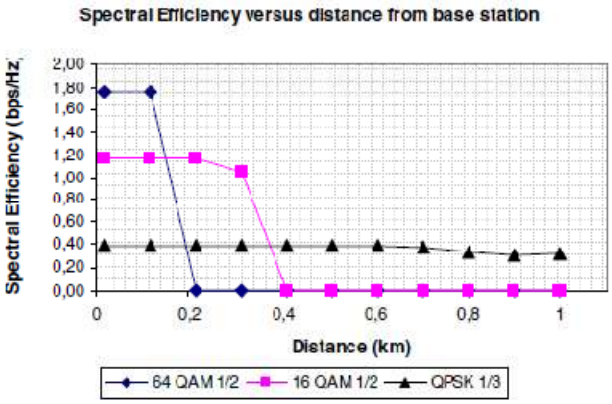

Figure 2-2 : Spectral efficiency in MBSFN [12]

MBSFN/MBMS and unicast transmission share the same frequency carrier, though it is also possible to have an independent carrier for MBSFN. Figure 2-2 shows spectral efficiency of MBSFN vs distance. Figure 2-3 illustrates the architecture of MBMS in the E-UTRAN. Two new network elements are introduced to control the service of MBMS.

The MBMS GW receives the Multimedia data packets from the Broadcasting Center and, in its PDCP layer, removes the IP header and compresses the packet. So for both single-cell and multi-cell transmissions in MBMS, the header compression is centralized and not handled by eNodeB. The user plane interface between MBMS GW and eNodeB is called M1 interface. To deliver downlink multimedia data packets, IP multicast is used to deliver packets over the M1 interface through M1 radio network layer [42]. There is no uplink data from eNodeB side on M1 interface. There is SYNC protocol function over the M1 interface that keeps the content synchronization for MBMS service data transmission. This feature allows that eNodeBs to identify the timing for radio frame transmission and detect packet loss [42]. In addition, There is a function in M1 interface that manages the IP multicast groups. The MBMS GW maintains the IP multicast groups.
A multicast group here refers to the eNodeBs that want to receive the Multimedia data content. The MBMS GW allocates the IP multicast group address. The eNodeB joins the IP multicast group to receive the MBMS User Plane data when the session starts and leaves the IP multicast group when the session ends [42].

MCE, Multicast Coordination Entity, allocates the same resource blocks for all eNodeB that are in MBSFN area [42]. MCE also selects the radio channel physical layer configuration (modulation and coding scheme) [42].
In the MBMS, the MCS selection process that normally is done by eNodeB is centralized and done by MCE. Thus, eNodeBs are only control RLC and MAC layers of their Radio Channels.
M2 and M3 Interfaces are pure Control Plane interfaces, used to carry the Signaling Message of a broadcast session between MCE and eNodeB / MME respectively.

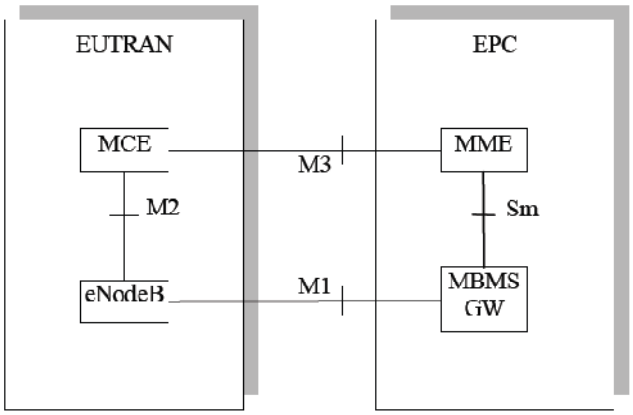

Figure 2-3 : General Architecture of E-UTRAN MBMS [41]

2.2.3 MBMS Physical and Transport Channel

In the LTE, users' data from the core network to UE passes through logical, Transport, and physical channels. Each channel is identified by the data type it carries. The Transport channel is located in MAC layer of eNodeB, while the physical channel is the actual Radio Air interface to UE.Figure2-4 shows different channels and their data types in the LTE. Multicast Traffic Channel, MTCH, is a point-to-multipoint traffic channel used in the downlink direction to deliver data content from core network to UE. At the same time, a point-to-multipoint MBMS control channel carries the control messages from core network to UE for one or more MTCH. In the MAC layer of eNodeB, two or more MTCH data can be multiplexed to a single MCH. This allows multiple MBMS services over a single MCH and increases efficiency. This method motivated the author to propose a Multicast Scheduler that increases the spectrum efficiency and results in the better streaming Qos. The detail of this scheduler is proposed in next section. One MCH only has data for one MBSFN area. When the transmission type is Single Cell in MBMS, the Multicast logical channel can be mapped to downlink share channel DL-SCH, but in the case of the MBSFN network, it is only mapped to MCH [27].

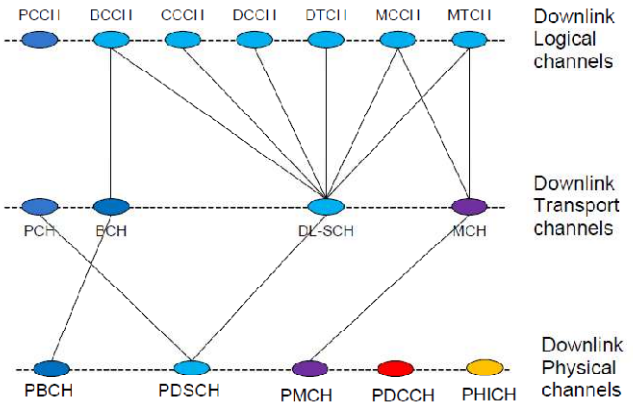

Figure 2-4 : LTE Downlink Channels [36]

2.2.4 LTE Frame

Each LTE frame consists of 20 subframes and length of each subframe is *0.5ms*. Depending on cyclick perfix length (short or long length) , each subframe consite of 6 or 7 OFDM symbole. The first three OFDM symboles are used for control channel and carry no data.

In frequency domain for 10Mhz bandwith ,each OFDM symbole have 1024 subcarriers , but because of preventing power leakage to the neighboring spectrum , only 600 subcarrier in the middle of spectrum are used to transmit. Each 12 consequative subcarriers are called a physical resource block or PRB. So for 10Mhz bandwidth there is 50 PRB that can be allocated to users. During scheduling a user , atleast one PRB is assigned to it.

2.3 Multipath Propagation

In a wireless channel, due to existence of different objects like building, trees and cars around the transmitter and the receiver, the signal from transmitter is diffracted and received through different routes with unlikely delays and phases and different attenuation coefficients. This causes the quality and utility of the information part of the received signal to degrade significantly. This effect is called multipath propagation. Moreover, transmitting a signal over a distance increasingly attenuates signal power (path loss effect). Thus, a radio receiver faces multiple attenuated and time-delayed versions of the transmitted signal, which also suffers from receiver thermal noise and some forms of interference from the other mobile transmitter. The signal, which has been received through different paths on the receiver, may add together constructively, improving the signal-to-noise ratio (SINR), or destructively decreasing the SINR. Usually, the effects of path loss and fading are modeled as a time-varying, linear filter with a limited number of taps.

2.3.1 Doppler Effect

Due to the mobility of the receiver, or even some of the received scattered signals, the Doppler Effect causes the observed frequency *f* of waves to differ in separate directions. This variation in frequency value, called the Doppler shift f_d, is proportional to the mobile velocity. For wireless propagation through the atmosphere, the wave's speed is equal to the speed of light *c*, and the observer receives the waves with a frequency *f*

$$f = f_c\left(\frac{c}{c \pm v_r}\right) = f_c\left(1 \pm \frac{v_r}{c \pm v_r}\right) \quad (2\text{-}1)$$

Where v_r is the speed of the source with respect to the medium, and *fc* is the frequency of wave scattered by the source. With relatively slow mobility, v_r is small in comparison to *c*, and the equation can be approximated to

$$f \approx f_c\left(1 \pm \frac{v_r}{c}\right) \quad (2\text{-}2)$$

More or less v_r is not constant over the time, and it is correlated to the angle between the mobile's velocity and its line of sight

$$v_r = v.cos\theta \qquad (2\text{-}3)$$

Where v is the receiver velocity with respect to the medium, and θ is the wave's angle of arrival with respect to the direction of receiver's motion. Replacing the v_r in the (2-3) gives

$$f = f_c\left(1 \pm \frac{vcos\theta}{c}\right) = f_c \pm f_d \quad , f_d = \frac{v}{c} f_c cos\theta = \Delta f_d.cos\theta \qquad (2\text{-}4)$$

Where Δf_d is the maximum Doppler shift spread that happens with $\theta = 0$ and f_d is Doppler shift. According to (2-4), the receiver always has a frequency in the range of

$$(f_c - f_d) \leq f \leq (f_c + f_d) \qquad (2\text{-}5)$$

2.3.2 Time Selectivity

The Doppler shift phenomenon can result in frequency dispersion. Fading value would also vary in the time because of Doppler spreading; therefore, the wireless channel behaves on a time selective manner.
Due to the time selectivity behavior of the channel, the channel model varies in time, and sometimes the receiver signal is not degraded. On the other hand, on some occasions, it may be strongly attenuated.

The time selectivity impact caused by the Doppler spread Δf_d depends on the ratio of the symbol duration T_s and the channel coherence time, where

$$T_{coh} \sim \frac{1}{\Delta f_d} \qquad (2\text{-}6)$$

To understand channel behavior, consider the following points:

- $T_s \,.\, \Delta f_d \gg 1$, the fading coefficients change during one symbol duration, and the channel is time selective. In this situation, channel estimation is not possible, and the only available solution for modulation scheme is non-coherent detection and differential modulation.
- $T_s \,.\, \Delta f_d \ll 1$, then it can be assumed the fading coefficient remains steady during a symbol duration, and channel is not time selective. Therefore, the receiver can use channel estimation, and for modulation we can apply coherent detection and normal modulation like QPSK, 16-QAM.

This behavior of the channel may be interpreted as fast or slow fading. In a wireless system, Doppler spreads frequency range between 1 to 100 Hz, corresponding to coherence times from 0.01 to 1s. In addition, symbol duration may vary from $2x10^{-4}$ to $2x10^{-6}$ s. [1] Thus, all symbols in a data block with 200 to 10^6 lengths are affected by more or less the same fading coefficient.

Therefore, when we model our system, we always consider during the transmission of a block; the fading is always constant, and we can assume a block fading.

2.3.3 Frequency Selectivity

Depending on the signal bandwidth *W* and the coherence bandwidth

$B_{coh} \sim \frac{1}{\Delta t_d}$ (2-7)

A wireless channel can be called wideband or a narrowband. Regarding the accuracy given by the sampling rate corresponding to the receiver bandwidth, the multiple received echoes of the transmitted signal are grouped in a cluster of inseparable components.

The sampling rate of bandwidth on the receiver side has a great role on the quality of signal. Usually, different copies and echoes of a transmitted signal are grouped together as unique signal. If the delay spread is significantly larger than the sampling time, the received signal is severely distorted. However, if the delay spread is not large compared to the sampling time, the multiple received copies of the transmitted signal will not significantly affect the signal.
A wireless channel from frequency selectivity point of view can be defined as follows:

- A non-frequency selective channel can be also called a flat or narrowband channel when $W \,.\, \Delta t_d \ll 1$. In this scenario, the wireless channel can be modeled by a single tap filter.
- A frequency selective channel can also be called a wideband channel when $W \,.\, \Delta t_d \gg 1$. The received signal consists of independent and separable copies of a transmitted signal. Therefore, the wireless channel can be modeled by a multi-tap filter.

Since the delays τ_k of each tap are different, some frequencies are not attenuated, while others may strongly be degraded by channel. If there are no significant differences between delays in unlikely paths, or if the differences are very small, then the delay spread attenuates all the frequencies the same way. Actually, the delay spread shows the speed of change of the mobile channel in the frequency domain.

Transmitting a multimedia signal over a wireless channel usually requires a high bandwidth. In practice, however, the bandwidth filter of the receiver side is band-limited, and the impulse response is modeled by limited number of tap.
N-tap delay channel can be modeled as

$h(\tau, t) = \sum_{n=1}^{N} h_n(t)\delta(\tau - \tau_n)$ (2-8)

Where

$h_n(t) = \sum_{l=0}^{M_n - 1} a_l(t) \exp(j\theta_k)$ (2-9)

Each multipath component arrives with a different delay, but if the delay spread of path is too long, then the arrival of the former symbol is not finished when the next symbol energy is initiated. The wideband channel can be modeled as a sum of several paths, and each path subject to non-frequency fading and has specific delays.

A large delay spread on taps results in a longer delay between the transmitter and receiver, so it would be beneficial to have more attenuation on each tap when the delay spread is long. The taps are usually assumed to be uncorrelated with each other,

The power profile of channel can be defined as function of delay spread of each tap

$$p(\tau, t) = |h(\tau, t)|^2 = \sum_{n=1}^{N} |h_n(t)|^2 \, \delta(\tau - \tau_n(t)) \qquad (2\text{-}10)$$

To characterize the power profile, we can mainly consider two parameters:

- Maximum delay spread $\Delta\tau$
- Root-mean-square (RMS) delay spread $\Delta\tau_{rms}$.

When the signal passes through a wireless channel whose RMS delay spread is much less than the symbol duration, we can expect inter-symbol interference, and the channel per tap can be assumed as narrowband.

2.3.4 Delay Spread

As shown above, an important parameter to model a wireless channel is the root mean square (RMS) delay spread $\Delta\tau_{rms}$, which is the standard deviation of the different delay paths.
It can be shown that random process with an average value depends on the distance and has standard deviation. Furthermore, it is a lognormal distributed and correlated to the shadow fading. [2]

According to [2], delay spread of wireless channel can be modeled as

$$\tau_{rms} = T_1 d^{\varepsilon} \mathrm{y} \qquad (2\text{-}11)$$

Where T_1 is median value of τ_{rms} at $d = 1\ km$ and ϵ is an exponential value that have range between 0.5 to 1and y is lognormal value in a way that $Y = 10\log y$ is Gaussian Random variable with zero mean and standard deviation σ_y that lies between 2 to 6db.
In addition, there is a negative relation between the delay spread and the shadowing coefficient. When the receiver is more shadowed, we expect the delay spread channel become larger. [2]

For a wireless channel, when the delay values per tap and power are given, the root mean square value of the delay spread $\Delta\tau_{rms}$ can be calculated as

$$\begin{matrix} tap\ delays\ \tau_i \\ tap\ power\ p_i \end{matrix} \quad \text{where i} = 1..\mathrm{N_{tap}}$$

$$\Delta\tau_{rms} = \sqrt{\sum \tau_i^2 \, p_i - (\sum \tau_i p_i)^2} \qquad (2\text{-}12)$$

2.3.5 TU6 Channel Model

The wireless channel model we have used in this Master thesis during the simulation is known as TU6 channel. [3]

In this model, the channel is characterized by 6 predefined power and delay taps. The maximum delay spread is more or less *5us*. Power distribution per tap is called Rayleigh Fading. The time and frequency response of TU-6 is illustrated on figure 2-5, 2-6 respectively.

Table 2-1 : TU-6 Channel Parameter

Tap	delay	Power	Fading Model
1	0.0	-3	Rayleigh
2	0.2	0	Rayleigh
3	0.5	-2	Rayleigh
4	1.6	-6	Rayleigh
5	2.3	-8	Rayleigh
6	5.0	-10	Rayleigh

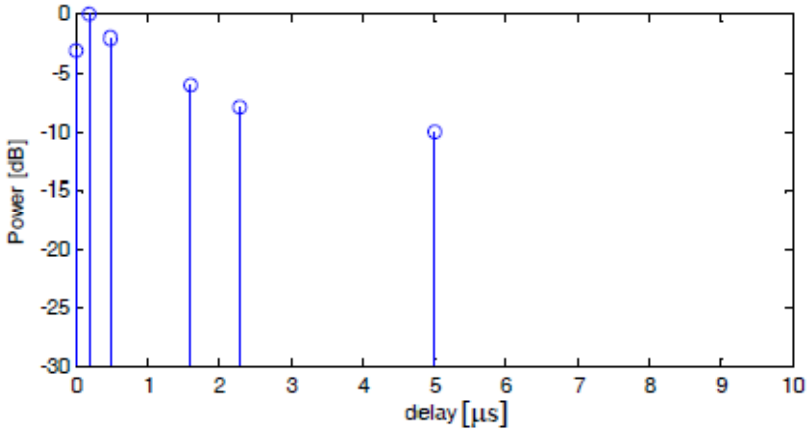

Figure 2-5 : Tu-6 Channel Impulse response

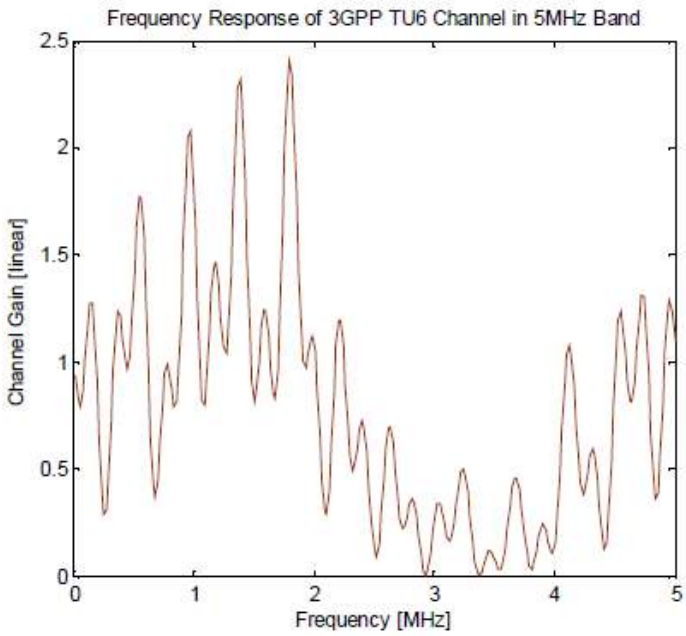

Figure 2-6 : TU-6 Channel Frequency response

2.3.6 Large scale propagation model

To model the behavior of the wireless channel on the large scale, two main factors—path loss and shadowing—are introduced.

2.3.6.1 Path loss models

The path loss model estimates the average attenuation of the transmitted signal over the propagation path with length of *d*.

In a free-space environment, the path loss L can be written as

$$P_L = \frac{P_{Rx}}{P_{Tx}} = \frac{G_{Rx}G_{Tx}\lambda^2}{(4\pi d)^2} \qquad (2\text{-}13)$$

Where G_{Tx} and G_{Rx} are the transmitter and receiver antenna gain respectively, P_{Tx} and P_{Rx} are the transmitted and received power. λ is the wavelength. If we want to have the path loss in dB, then (2-13) changes to

$$P_L(d) = L_0 - 20log_{10}d \qquad (2\text{-}14)$$

L_0 is a parameter that depends on the frequency and the antenna height. The actual wireless propagation is not done through free-space, and several studies offer a real path loss model in urban and suburban areas. The most widely used model is the Okumura-Hata model. [4] The Walfisch-Bertoni model [5] is useful to model outdoor radio propagation for applications in urban areas at 900 and 1800 MHz bands.

In addition to the distance, the path loss depends on the propagation environment. α shows the dependency of the path loss to propagation environment:

$$P_L(d) = L_1 - 10\alpha log_{10} d \qquad (2\text{-}15)$$

Similar to L_0, L_1 is a constant term that depends on the antenna gains, frequency etc.
The parameter α is known as path loss exponent, and depending on the propagation environment, it can differ from 2 to 6. [6]

The path loss model that has been used in this simulation is

$$P_{L\_db}(d) = 128.1 - 36.7 log_{10} d \qquad (2\text{-}16)$$

2.3.6.2 Shadow Fading

Path loss gives an average received power in the distance *d*. Moreover, an additional random variable component with lognormal distribution is always added to fit the propagation model. [7]

The propagation loss is extended to

$$P_L(db) = 128.1 - 36.7 log_{10} d + X_S \qquad (2\text{-}17)$$

Where X_s is random variable and has Gaussian distribution with zero mean and standard deviation σ_s.

$$p(X_S) = \frac{1}{\sqrt{2\pi\sigma}} exp(\frac{-X_S^2}{2\sigma_S^2}) \qquad (2\text{-}18)$$

Figure 2-7 illustrate the shadow fading and pass loss effect on the received power. Obstacles like buildings, cars, mountains, trees, etc. cause shadow fading in the propagation path between the transmitter and the receiver.

Common values for standard deviation of shadow fading are between 5 to 12 dB. [8] In this Master's thesis, a shadow fading with standard deviation of *8dB* is considered.

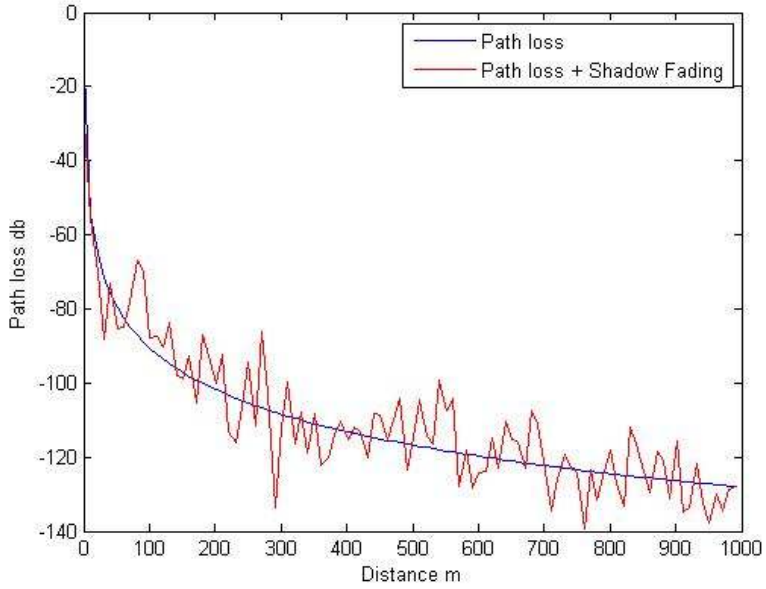

Figure 2-7 : Large scale propagation model

2.3.7 Calculation of SINR in OFDM

The SINR of each node needed to be reported to eNodeB as input parameter for scheduling algorithms.

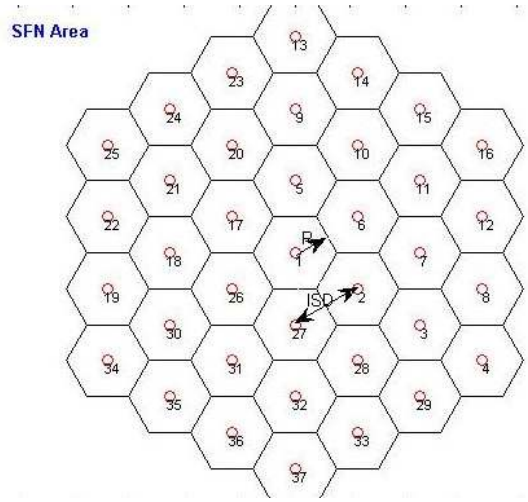

Figure 2-8: Wireless Network area

In the simulation model, all the UEs are located on central cell and receive signals from the neighboring cells. When the cells transmit the unicast OFDM, all the receiving signals (other than central cell) are considered destructive interference. [12] However, the case is different in an MBSFN scenario.

In the MBSFN, the role of the arriving signal as either constructive or destructive interference depends on delay of arrival. [12] The portion of received signals with delay less than or equal to cyclic prefix length are considered constructive interference. Simply put, it will add to the signal gain.
The impact of the received signals from an eNodeB is therefore related to the propagation delay. If the distance of UE_i to central cell and $cell_i$ is r_0 and r_i respectively, then the propagation delay can be formulated as

$$\tau_i = \frac{r_i - r_0}{C} \quad , where\ C\ is\ speed\ of\ light \tag{2-19}$$

The constructive portion of received signal from each eNodeB is a weight function of the propagation delay. [13]

$$w = \begin{cases} 0 & \tau < -T_u \\ 1 + \frac{\tau}{T_u} & -T_u \le \tau < 0 \\ 1 & 0 \le \tau < T_{CP} \\ 1 - \frac{\tau - T_{CP}}{T_u} & T_{CP} \le \tau < T_{CP} + T_u \\ 0 & otherwise \end{cases} \tag{2-20}$$

Where T_u is useful signal length and T_{CP} is Cyclic Prefix length.

Due to different multipath channel delays, signals arrive at different intervals. One important issue during SINR calculation is locating the FFT window or simply saying where to start sampling the received signal. [14] There are three approaches. One approach locates the FFT window upon arrival of first path. Another approach locates the FFT window upon the start of highest arrival signal, and the third always synchronizes to the first cell's signal arrival. Due to simple implementation in the simulation system, the central cell is used as a reference time to start the FFT window. Therefore, there is no case of propagation delay less than a useful signal length.

Despite propagation delay, multipath propagation channel delay also affects whether the received signal is constructive or destructive. [12] The weight function should consider the total delay of each fast fading path, as well as the propagation delay.

With an SFN area that consists of N cell and modeling the propagation channel with M tap filter, we can formulate the received SINR for each user within the central cell as [12]:

$$SINR = \frac{\frac{\sum_{i=0}^{N}\sum_{j=1}^{M} w(\tau_i + \delta_j) * P_j}{q_i}}{\sum_{i=0}^{N}\sum_{j=1}^{M} \frac{\left(1 - w(\tau_i + \delta_j)\right) * P_j}{q_i} + N_0} \tag{2-21}$$

Where $\tau_i(m)$ is the propagation delay for base station i (for base station 0, $\tau 0(m)=0$), δj is the additional delay caused by path j. P_j is the average power associated with the j-th path and can be modeled.

$$P_j = 10^{(P_{Tx(db)} - P_{L_{channel\ j}})/10} \quad (2\text{-}22)$$

q_i is path loss associated with distance d from UE position to Cell i. We have already shown q follows a model as:

$$qi\ (\mathrm{d}) = 10^{(128.1 - 36.7 log_{10} d + X_S)/10} \quad , where\ d\ is\ distance\ between\ UE\ and\ Cell\ i$$

Where X_s is shadow fading component. The shadow fading factor for each UE can be modeled in a way that is comprised of two components [12]: a common component that belongs to all eNodeB, and a second component that relates specifically to eNodeB.

$$X_{s_i} = a\epsilon + b\epsilon_i \ \ where\ a = b = \frac{1}{\sqrt{2}} \quad (2\text{-}23)$$

Where ϵ and ϵ_i are random variables with a Gaussian distribution with zero mean and variance $var(\epsilon_i) = var(\epsilon) = \gamma^2$. [15] In the simulation system, we have considered
$\gamma = 8db$.
Considering (2-21), the SINR formula can be reformatted as [12]

$$SINR = \frac{\frac{\sum_{i=0}^{N}\sum_{j=1}^{M} w(\tau_i + \delta_j) * P_j}{q_i}}{\sum_{i=0}^{N}\sum_{j=1}^{M} \frac{(1 - w(\tau_i + \delta_j)) * P_j}{q_i} + N_0 10^{a\epsilon/10}} \quad (2\text{-}24)$$

Where q_i should be considered as:

$$q_i\ (\mathrm{d}) = 10^{(128.1 - 36.7 log_{10} d + be_i)/10} \quad (2\text{-}25)$$

2.4 Scalable Video Coding

Scalable video Coding (SVC) has been an attractive solution for Multimedia streaming and there have been a lot of studies on that since 20 years ago [54]. A video stream is called scalable when part of its bit stream is removable in order to adapt the bit rate to Network condition i.e. Received power, user preference and demanded quality of pictures or Display terminal capabilities [54]. The new sub stream with removed bit rate, form a valid decodable stream that the quality is less than complete bit stream but still high when compare it to remaining data stream [54]. In this Master thesis, when the video stream cannot form a new sub stream by removing some part of its bit rate it is referred as *Single layer stream*.

The common modes of scalability are temporal, spatial, and quality scalability [54].In the spatial scalability the subset contain the picture with reduced size comparing to original picture and a sub stream with temporal has less frame rate less than original bit stream [54].The subset stream

keeps the same picture size and frame in quality scalability but with lower signal to noise ratio or fidelity, that is why it usually called SNR scalability [54].

In the high level design of SVC, The H.264/MPEG4-AVC components are used as compatible with standard [55]. The components like motion-compensated and intra prediction, the transform and entropy coding, the deblocking , the NAL unit packetization (NAL – Network Abstraction Layer)are still kept in the SVC-coder[55]. The base layer of an SVC bit-stream can be compatibly coded with H.264/MPEG4-AVC standard therefore the base layer of SVC bit-stream can be decoded by all H.264 coder. In the SVC-coder, new components are added to support spatial and SNR scalability [55]. Figure 2-9 show the code structure with two quality layer.

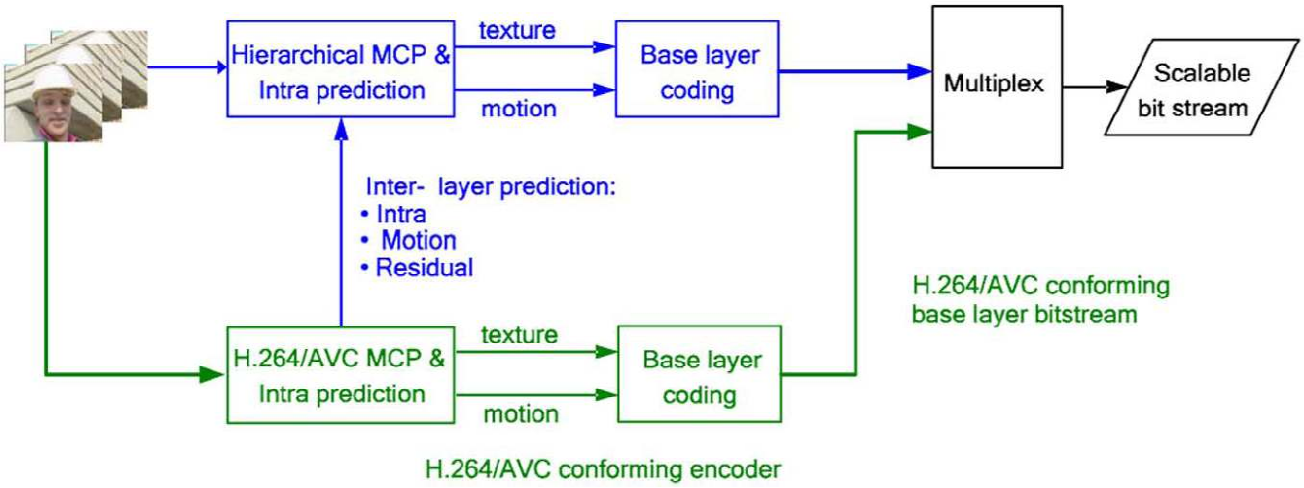

Figure 2-9: Coder structure with two quality layers [60]

The structure of H.264/AVC is divided to two parts: *Video Coding Layer (VCL)* and *Network Abstraction Layer (NAL)* [54]."The packet of VCL represent coded source stream while the NAL formats these data and provides header information" [54].

2.4.1.1 Network Abstraction Layer

The coded video streams are divided to NAL unit. The length of NAL packet is an integer number of byte with one byte header in the beginning and payload. NAL units are two types : VCL NAL units, which contain coded slices or coded slice data partitions, and non-VCL NAL units, which contain associated additional information like parameter sets and Supplemental Enhancement Information (SEI).[54] The information of non-VCL NAL unit can be used during decoding process and used for bit-stream manipulation[54].

2.4.1.2 Video Coding Layer (VCL)

In the H.264/AVC coder, the pictures are chopped to smaller coding units called slice or macroblock[54]. Macroblock in video stream is a rectangular area with spatially or temporally predicted chroma sampling format [54]. Each macro block are coded independently. H.264/AVC supports three basic slice coding types [54]:

- "I-slice: *intra-picture* predictive coding using spatial prediction from neighboring regions.
- P-slice: intra-picture predictive coding and inter-picture *predictive* coding with one prediction signal for each predicted region.
- B-slice: intra-picture predictive coding, inter-picture predictive coding, and inter-picture *bipredictive* coding with two prediction signals that are combined with a weighted average to form the region prediction".

2.4.2 Temporal Scalability

The typical temporal scaling is based on temporal decomposition by using hierarchical B-picture [60].
Fig 2-10 shows hierarchical B-pictures with two layers of SNR fidelity scalability, base layer and one enhancement layer. Pictures with labels T0 represent *key pictures*. These pictures are used for synchronization reference between encoder and decoder. As Fig 2-10 shows , the enhanced layer of other two T0 pictures are inter-predicted from the preceding base layer pictures labeled with T0 [60]. The temporal enhancement levels are the B-pictures between two consecutive key pictures. Where T1 pictures form the first temporal enhancement to the key pictures and pictures labeled T2 form the second temporal enhancement [60]. The T1 and T2 base layer pictures predicted from the highest available enhancement layer pictures. This approach is also known as medium granularity scalability (MGS).

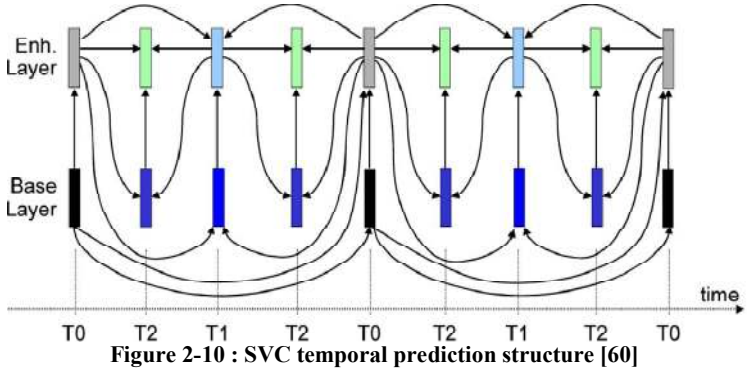

Figure 2-10 : SVC temporal prediction structure [60]

2.4.3 Distortion Model of Multilayer stream

The main purpose of this Master thesis is to examine performance of different scheduling algorithms in delivering the scalable video coding stream. A main factor to consider in regards to the performance of delivered stream to the users is the distortion and PSNR of the received of stream.

Distortion in the stream is caused by two components [22]: source distortion, which is introduced by quantization during coding, and channel distortion, which is introduced when the transmitted packets are lost. The final distortions are a sum of the mentioned components. The coding rate can be adapted according to user SINR and demanded quality of picture [23], so if the user SINR

falls down, the coding rate can also be forced to a lower level to make it possible for the user receives the stream with a lower quality. But in our simulation system, there is no feedback system from user SINR to MANE [23]. The scheduling only tries to minimize the channel distortion [22], and the source distortion is always the same for each stream, never updated upon the user SINR.

The distortion model in the simulation system for all 8 test streams is introduced in [22].

Table 2-2: Parameters of the distortion model for the test sequences [22]

qb=(38,32,26)	ρ_1	ρ_2	ρ_3	ρ_{total}	D_1	D_2	D_3	α	β
Crew	130.3	211.1	460	801.4	50.8	26.2	11.5	56.5	442
Foreman	88.5	167.3	339	594.9	48	23.4	10	83.1	614
Hall	45.4	104.7	236.6	386.7	34.2	18	8.8	21.5	150.9
Harbour	134.1	302	637.6	1073.7	95.9	45.1	19.8	58	644.1
Mobile	200.4	402.3	736.7	1339.4	124.7	52.2	21.3	146.8	1742.4
Mother	29.1	71.9	165.8	266.9	24.1	13	5.1	16.3	98.9
News	60.2	120.1	238.1	418.4	36.3	17	6.3	33.6	232.8
Soccer	127	198.3	454.4	779.8	52	27.9	11.1	122.4	923.8

Each test stream consists of one basic layer and two enhancement layer.

Consider p_i as probability of packet loss in layer i,($i=1,2,3$). Aside from the basic layer, the packet loss on the enhancement layer can be caused either by direct packet loss of the enhancement layer itself, or by missing a dependent packet from a lower enhancement layer.
The total packet loss of each layer can be formulated as [22]:

$$\pi_1 = P_1 \qquad (2\text{-}26)$$
$$\pi_2 = \pi_1 + P_2 - \pi_1 P_2 = P_1 + P_2 - P_1 P_2$$
$$\pi_3 = \pi_2 + P_3 - \pi_2 P_3 = P_1 + P_2 + P_3 + P_1 P_2 + P_1 P_3 + P_3 P_2 - P_1 P_2 P_3$$

It should be noted that packet loss on the basic layer causes a severe loss on all layers, degrades the quality, and increases distortion. According to [24, 22], the distortion linearly increases with basic layer packet loss unless$P_1 \leq 0.1$.

By introducing parameter α in the distortion model of each stream, it is possible correlate the packet loss probability of basic layer to the actual, achieved distortion of layer one during a simulation with a different qb. [22]

$$D_{C,1} = \alpha\sqrt{D_1}P_1\,, \;\; while\; P_1 < 0.1 \qquad (2\text{-}27)$$

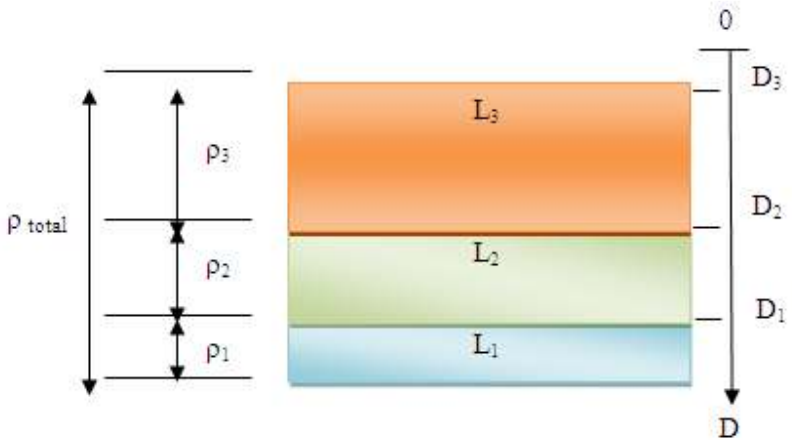

Figure 2-11 : Encoding rates and distortions for SVC video [22]

Figure (2-11) shows the scalability feature of an arbitrary video stream. In the proposed model [22], if all the packets of layer 3 are delivered error-free and can be decoded, then the total distortion of system decreases by D_2-D_3. However, if some packets are lost byπ_3, then the total distortion decreases by $(D_2 - D_3)(1 - \pi_3)$. This means that channel distortion due to packet loss in layer 3 is$(D_2 - D_3)\pi_3$. Therefore, assuming $P_1 < 0.1$, total channel distortion can be formulated.

$$Dc = \alpha\sqrt{D_1}P_1 + (D_1 - D_2)\pi_2 + (D_2 - D_3)\pi_3 \qquad (2\text{-}28)$$

$$Dc = \beta P_1 + (D_1 - D_3)P_2(1 - P_1) + (D_2 - D_3)P_3(1 - P_1)(1 - P_2) \qquad (2\text{-}29)$$

$$where\ \beta = \alpha\sqrt{D_1} + (D_1 - D_3)$$

Since we have assumed that video streams with more than 10% packet loss in the basic layer are undesirable, the maximum channel distortion is achieved when the basic layer packet loss is equal to 10% and there is full packet loss on all enhancement layers.

$$D_{C_{Max}}(P_1 = 0.1, P_2 = 1, P_3 = 1) = 0.1 \times \alpha\sqrt{D_1} \qquad (2\text{-}30)$$

The values of parameters for different test stream are shown in Table (2-31).

2.4.4 Distortion Model of Single layer video stream

It is expected that source distortion of single layer stream would decrease exponentially as coding rate increases [22, 26]. For the test stream, if we assume the encoding rate of single layer video stream is equal to total coding rate of layer one to tree, then distortion changes to [22]

$$D_{Single}(\rho_{total} = \rho_1) = \gamma\rho_{total}^{\epsilon} \qquad (2\text{-}33)$$

γ, ϵ Are Stream dependent values that can be found in Table (2-3).

Table 2-3 : Single layer distortion model parameters

Stream	ρ_{total}	γ	ϵ
Crew	801.4	5784.3	-0.972
Foreman	594.9	5644.2	-1.063
Hall	386.7	619.2	-0.759
Harbour	1073.7	6722.4	-0.868
Mobile	1339.4	49052.5	-1.127
Mother	266.9	655.7	-0.98
News	418.4	7568.9	-1.303
Soccer	779.8	9699.6	-1.079

$$Dc_{Single} = \alpha\sqrt{D_{Single}}\,p_{Single} \qquad (2\text{-}34)$$

3 System Model

3.1 Network Architecture

3.1.1 MBSFN Area

The MBSFN area is modeled as cellular network as hexagonal topology with eNodeB at the center of each cell. Each cell is surrounded by six neighboring cells. An omni-directional antenna is assumed for each site. A key parameter to concern is the number of cell tiers around the central cell. The tier number will affect total SFN cells available for scheduling, and it will affect the user SINR.

The total number of SFN cell is increasing sharply by the increasing the number of Tier N_{Tier}.

$$N_{Total\ SFN\ Cell} = 1 + 3N_{Tier}(N_{Tier} + 1) \qquad (3\text{-}1)$$

In the MBSFN network, if we assume a perfect synchronization among all eNodeBs, the maximum distance at which the received signal can be considered fully constructive correlates to the cyclic prefix length and speed of light. As (2-20) says, the signals with propagation delays less than the cyclic prefix are fully constructive signal.

$$for\ \tau < T_{CP}\ , if\ T_{CP} = 16.6\mu s$$
$$Distance\ with\ constuctive\ Arrival\ Signal = T_{CP} * C = 16.37\mu s * 3 \times 10^{8} = 4913\ m$$

If we assume an inter-site distance of 1.5km after the third tier, part of the signal becomes destructive. Moreover, according to (2-20), after a certain distance, an arrival signal becomes completely destructive and has no gain on SFN.

$$Max\ Distance\ with\ constuctive\ Arrival\ Signal = C \times (T_{CP} + T_u) = 25km$$

With ISD=1.5km, one can approximate no useful information from the arrival signal on tier 15. However, due to path loss, distance of eNodeB and UE tremendously degrades the arrival signal, so signals from tiers 10 and 11 are so weak that they have no impact on the user SINR. In addition, increasing the number of tiers increases the simulation time. On the other hand, it does not have much effect on the SINR, which is an important factor for scheduling decisions.

Figure (3-1) shows the CDF of SINR. By increasing the number of tiers from 5 to 6 and more, a significant increase can be seen on SINR, but it results in longer computations and simulations plus SINR greater than 20db doesn't have any effect on the simulation. We have used a total number of 5 tiers around the central cell to structure our MBSFN area.

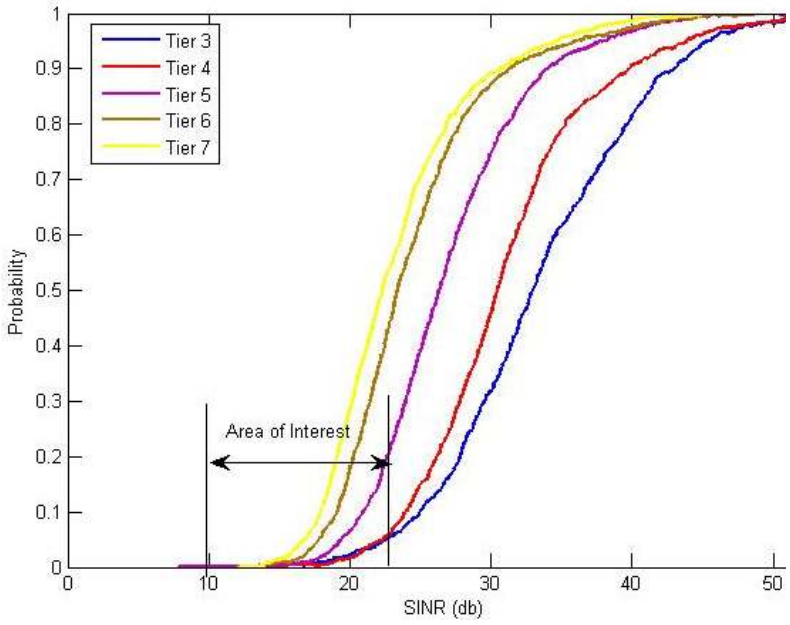

Figure 3-1: users SINR distribution

The desired SINR threshold is around 20 dB (because of SINR to CQI mapping), becuase the user can benefit the highest code rate and modulation. It is mainly important to see the probability of SINR exceeding 20 dB, because thereafter 20 db there is no higher MCS (Modulation and coding scheme) is available to transmit. To make the simulation less time consuming, we ignore the increase of SINR with 6 tiers, subsequently using 5 tiers with a total of 91 SFN cells to form the MBSFN Area.

3.1.2 User Distribution

In the simulation system, all users are distributed on the central cell and moved according to the mobility scenario. The number of users depends on the total number of multicast groups. During simulation initialization, for each multicast group, the subscriber number is a random number between 1 and 8. Finally, the users of all multicast groups, regardless of their assignee group, are distributed uniformly around the central cells.

It should be noted that, according to 3GPP simulation setup parameters, the minimum distance between UE and eNodeB should be 50m. [21]

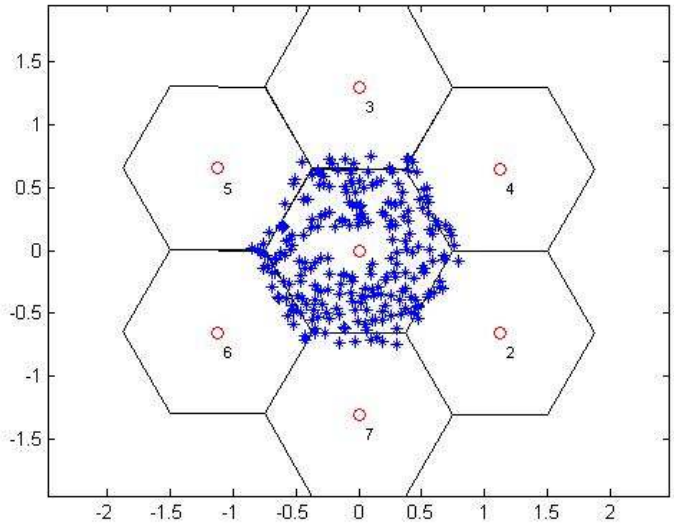

Figure 3-2 : Users Distribution

3.2 User Mobility Scenario

A key parameter to the scheduling algorithm is the user's SINR in each multicast group. Users should move within the cells in order to experience different SINR, then the robustness of the algorithm against SINR changes is tested. However, in the simulation system, since the users are distributed in on cell, it is not possible to have a mobility scenario like [3], due to the impossibility of moving the users at that speed in the limited simulation environment area.
Another interesting issue to consider is that, during the scheduling, the overall SINR of each multicast group is important. This means that, even if the users move to another cell during the simulation (which is not possible on this model), the final SINR distribution of total users will follow exactly the same as Figure (3-1).The possibility of each multicast group experience with a different SINR status is the same when the users are distributed on central cells and moved randomly within the cells or intra-cells.

During simulation, each user is randomly chosen to go right or left with a predefined speed of 1m/s. When the user approaches the edge of the cell, it is randomly chosen to move up or down in relation to the cell. The second time the user approaches the edge, if the user is on the left part of the cell; then is forced to move to the right and vice versa.

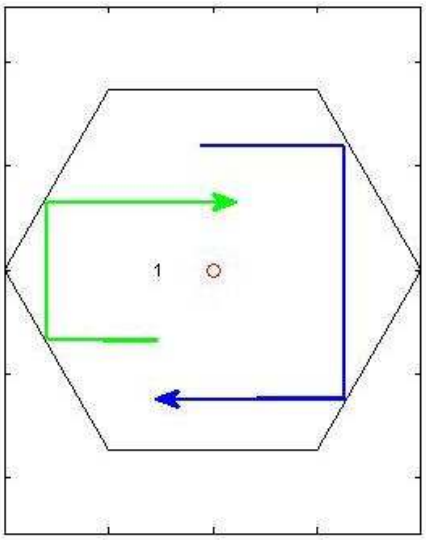

Figure 3-3 : user mobility scenario

In this mobility scenario, users somehow experience more or less every part of cell, and one can claim overall SINR of multicast groups are the same. However, in each TTI, users may experience different SINR values.

3.3 SINR Mapping

In the LTE, subcarriers are assigned to users in the chunks called physical resource blocks (PRBs). Upon receiving the signal, the UE should report its SINR to eNodeB via upload control channel. In the next scheduling opportunity, the base station assigns the highest modulation and coding Scheme to UE according to its reported SINR.

To reduce the enormous feedback overhead and compress the control data, the UE can report to eNodeB with the channel quality indicator (CQI), a mapped version of SINR, in two ways: aperiodic feedback and periodic feedback. [16]

“In aperiodic feedback, the UE sends CQI only when it is asked to by the BS. On the other hand, in periodic feedback, the UE sends CQI periodically to the BS; the period between 2 consecutive CQI reports is communicated by the BS to the UE at the start of the CQI reporting process” [16].

Moreover, the UE can report CQI at “different frequency granularities in aperiodic CQI feedback” [16]. In *Wideband feedback*, the UE reports one wideband CQI value for the whole system bandwidth. In this Master thesis, we have considered a periodic wideband CQI scenario.

Each UE is located in different position within the SFN area and owns a frequency selective channel response. Moreover, the PRBs (subcarrier) assigned to each UE are in different parts of

the frequency band. In [15], a simple method of achieving effective SINR from OFDM subcarrier for different modulation and coding Scheme is introduced.

$$SINR_{effective} = -\beta \frac{1}{N}\sum_{i=0}^{N-1} e^{\gamma_i/\beta} \quad where\ \gamma_i\ is\ the\ SINR\ of\ Subcarrier\ i \qquad (3\text{-}2)$$

β Is a calibration parameter that is used to fit the $SINR_{eff}$ and Theoretical BER curve together.

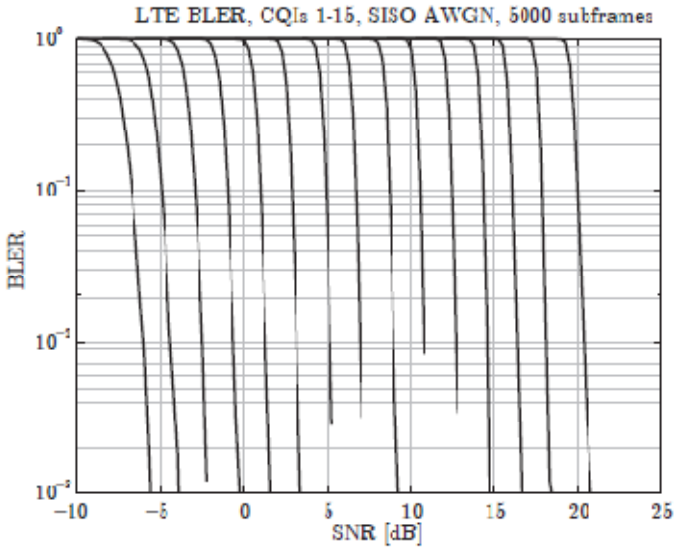

Figure 3-4 BLER Vs SINR for different MCS [18]

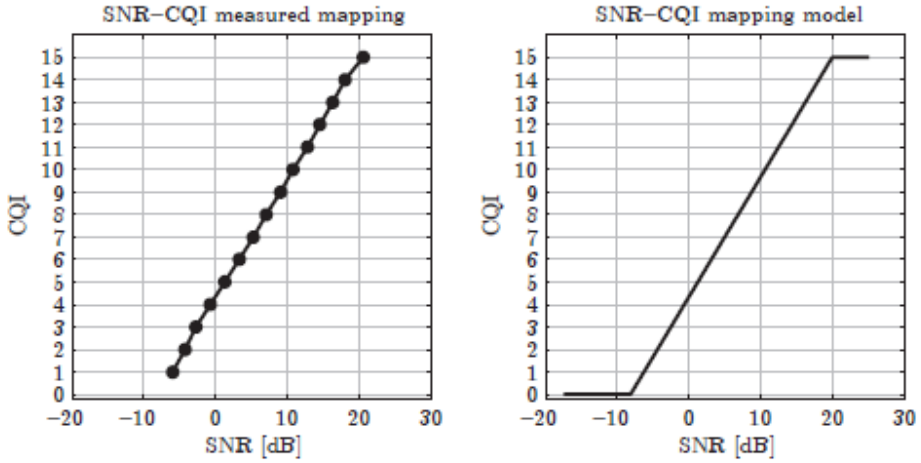

Figure 3-5 : SINR to CQI mapping [18]

For each modulation and coding Scheme (MCS), β is chose in a way the effective SINR can be fitted to its corresponding BLER curve. The BLER curve is different for different bandwidths and depends on the existence of HARQ. [18]

If we assume all the subcarriers on the LTE frame are modulated and presume all subcarriers assigned to UE experience the same fading channel, then according to [12,19], we can assume that the calculated SINR is independent of the subcarrier and is the same for all.

In this case, there is no further need to map SINR to effective SINR and calibration. To map the SINR to CQI, we have used a simple method of table mapping for 15 MCS. [18] .

Table 3-1 : SINR to CQI Mapping table

CQI	Modulation	Efficiency bit/Hz	SINR db
1	QPSK	0.1523	-5.6
2	QPSK	0.2344	-3.85
3	QPSK	0.377	-2.1
4	QPSK	0.6016	-0.35
5	QPSK	0.877	1.4
6	QPSK	1.1758	3.15
7	16QAM	1.4766	4.9
8	16QAM	1.9141	6.65
9	16QAM	2.4063	8.4
10	64QAM	2.7305	10.15
11	64QAM	3.3223	11.9
12	64QAM	3.9023	13.65
13	64QAM	4.5234	15.4
14	64QAM	5.1152	17.15
15	64QAM	5.5547	18.9

During mapping SINR to CQI ,as figure 3-4,3-5 shows , one can decided for BLER rate of each SINR threshold . In order to get rid of packet loss due to channel error impact on simulation we have set the BLER threshold around 1% .In the simulation system, at each TTI, all the UEs calculated their SINR and map it to the corresponding CQI and report it to main scheduler.

3.4 User Utility

The main duty of the scheduler is to minimize the total distortion of the delivered stream. This premise can be achieved by reducing the channel distortion. On the other hand, the algorithm should always schedule a multicast group that, with the fewest transmission resources, would result in higher quality pictures or less distortion.

As mentioned earlier, during the scheduling, the source distortion of a stream is neglected, and if all packets are delivered error-free or the user's average throughput in the multicast group is equal to total coding rate, the distortion component is zero.

As we discussed earlier, when a share of upper enhancement layer packets are delivered error-free, while packet loss of the basic layer packet loss is still less than 10%, the total distortion decreases accordingly. Therefore, the more the enhancement layer is scheduled in multicast groups, the more distortion decreases, allowing users to benefit from better picture quality.

User utility is a number between [0, 1] and introduces the status of total distortion in the delivered stream. When user utility approaches 1, it shows the total distortion due to channel distortion or packet loss falling to 0. [22] for multilayer stream , utility is modeled as :

$$U(r_1, r_2, r_3) = \begin{cases} 1 - \frac{D_C(P_1, P_2, P_3)}{D_{Cmax}} & r_1 > 0.1 \ (p_1 < 0.1) \\ 0 \end{cases} \qquad (3\text{-}3)$$

Packet loss of each layer can be obtained

$$p_i = 1 - \frac{r_i}{\rho_i} \qquad (3\text{-}4)$$

When r_i is the average received throughput in the layer i and ρ_i is coding rate.

For the single layer video has bit rate equal to total coding rate of SVC layer. The utility is briefed to

$$U_{Single}(r) = \begin{cases} 1 - \frac{Dc_{Single}(r)}{Dc_{Single\_max}} & r > 0.1 \ (p < 0.1) \\ 0 \end{cases} \qquad (3\text{-}5)$$

In each TTI, the scheduler selects the layer that its gradient of user utility curve $\frac{\partial u}{\partial r_i}$, is maximized. The gradient of utility curve lets the scheduler decide, regardless of what has happened before.

3.5 Buffer Model

Streaming can be offline or real-time. In offline streaming, the scheduler has access to as many data stream packets as it wants (stream video files are stored on a local server hard disk), and usually during the data burst transmission, it uses the maximum rate (PRB=50). Thereafter we refer to offline streaming as "full rate Transmission."

On the other hand, streaming is always real-time. Therefore, the packets are stored on buffer with limited length. The scheduler only sends the bytes that are stored on the buffer between two occasions of scheduling the same layer of a group. Thus, for transmitting small data bursts, the scheduler does not use all available resources, and some PRBs still remain unused. Moreover the performance of scheduler in real-time mode is considerably lower than offline mode. (The reason

is reviewed on chapter 6). Available empty resources (PRB groups) motivate the proposal of the Multi Group-Max_sum algorithm. This scheduler aggregates different stream packets to a larger packet and multicasts it to the network. The encapsulated packet would be opened, and unrelated packets for each group would be dropped. The challenging part of this scheduling is deciding the highest MCS that minimizes frequency resource usage of each group, while at the same time maximizing the total utility function of multicast group's users.

3.6 Summary

The table 3-2 summarizes the system model during simulation.

Table 3-2 : System model parameters

Parameter	Value
Cellular Topology	5 Tier around Central cell
Inter Site Distance	1.5 Km
System Bandwidth	10 MHz, 50 PRB
Channel Model	TU6-Urban
Propagation Model	$P_L(db) = 128.1 - 36.7log_{10}d + X_S$
Shadow Fading	8db
Noise Figure	9db
Cyclic Prefix	16.67μs
OFDM Symbols for data each TTI	9 of 12 symbol
MCS	Table 3-1
Stream Distortion model	Table 2-2,2-3
TX power	46dbm

4 Scheduling Algorithms

4.1 Introduction

The simulation implements four different scheduling algorithms. There are other combinations of multicast scheduling algorithms [22] that we do not cover here. In the following section, we present the details of each scheduling algorithm. It should be noted that some parts of scheduling algorithms, like layer and rate selection and assigning the number of PRB, are common for all.

4.2 Max-Prod Scheduling Algorithm

During simulation, there are some assumptions:

1) Initially, 20ms of data flow for each multicast group are stored on the separate buffer.
2) We begin with the assumption that all users are saturated at the basic layer.(The average throughput of basic layer is equal or greater than coding rate).

Max–Prod Scheduling algorithm was proposed for HSDPA and LTE [22, 25], and at each timeslot n, it maximizes the product of users utility, $\varphi(n) = \prod_{m=1}^{M} \prod_{S=1}^{S_m} u(m,s)$ within the multicast groups, where S_m is the total number of users in a multicast group and M is number of multicast groups. As discussed earlier, $u(m,s)$ is the utility function of user s in the multicast group m and depends on received throughput for packet loss rate.

In the simulation, at each timeslot the scheduler tries to select the multicast group, layer and transmission rate that maximize the gradient of $\varphi(n)$ curve or $(n) - \varphi(n-1)$. For the detail of achieved gain in each scheduling decision, one can refer to [22].

Before deciding, the scheduler should know the current SINR of each subscriber in multicast group. It is assumed that there is no delay in report of SINR to the eNodeB.

Despite the SINR, the scheduler should be aware of users' average throughput for each layer in multi cast groups. It is not possible for UE to provide continuous feedback on its average throughput for each layer to eNodeB, but the scheduler can estimate the current value of layer throughput of each subscriber. In the simulation, there is no acknowledgment feedback from the user to inform the eNodeB that packet is delivered, but the threshold of SINR mapping to CQI is set in a way that guarantees the packet with a defined transmission scheme is delivered to UE with more than 99% success. Therefore, it is optimistic to neglect the 1% of failure and assume that, if the eNodeB schedule the packet has the defined transmission scheme, the packet is not lost and delivered to multicast group.

Let consider $u_n^k(m,s) = {}^{\partial u(m,s)}/_{\partial r_k}$[22].

In the first step, the scheduler should determine the highest transmission modulation and coding for each multicast group. The transmission rate depends on whether the scheduler works on a full-rate transmission or a limited-to-buffer data rate.

In the real-time scenario, the number of bytes that are stored on the buffer can be determined by

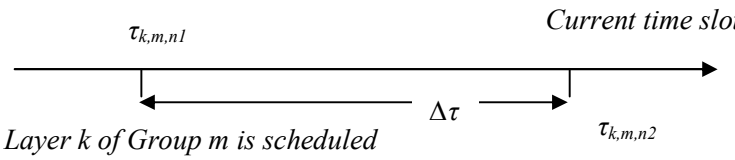

$$PRB_{buffer} = Max\left\{1, \frac{(\tau_{k,m,n2} - \tau_{k,m,n1}) \times Stream\ coding\ rate}{OFDM\ symbole\ for\ data\ per\ sub\ frame * bit\ per\ symbol * code\ rate}\right\} \quad (4\text{-}1)$$

$$R_{MCS} = PRB_{buffer} \times OFDM\ symbole\ per\ frame * bit\ per\ symbol * code\ rate \quad (4\text{-}2)$$

And for the full-rate transmission rate, the scheduler use the full resource allocation

$$R_{MCS} = PRB_{full\ rate}(50) \times OFDM\ symbole\ per\ sub\ frame * bit\ per\ symbol * code\ rate \quad (4\text{-}3)$$

The bit per symbol and code rate for each MCS index can be found in table (3-1). The MCS is index of the maximum value of (4-4).

$$MCS^*_{k,n}(m) = argmax_{1 \le MCS_{index} \le 15}\left\{\sum_{s=1}^{S_m} \frac{u_n^k(m,s)}{u_n(m,s)} . R_{MCS}\right\} \quad (4\text{-}4)$$

After deciding the transmission rate and MCS index, the second step occurs when the scheduler selects the video layer that maximizes the product of user utility per multicast group.

$$\boldsymbol{k_n}(\boldsymbol{m})^* = argmax_{1 \le k \le L}\left\{\sum_{s=1}^{S_m} \frac{u_n^k(m,s)}{u_n(m,s)} . {R_{MCS}}^*\right\} \quad (4\text{-}5)$$

The final step is to decide the multicast group with the selected layer and transmission rate that have the highest product of users' utility value.

$$\boldsymbol{m_n^*} = argmax_{1 \le m \le M}\left\{\sum_{s=1}^{S_m} \frac{u_n^{k^*}(m,s)}{u_n(m,s)} . {R_{MCS}}^*\right\} \quad (4\text{-}6)$$

The output of the scheduling algorithm is now decided, and it passes the scheduling parameters (MCS, PRB, Multicast group, $\boldsymbol{m_n^*}$, and scheduling layer $\boldsymbol{k_n}$) to the main loop of the simulation.

4.3 Max_Sum Scheduling Algorithm

All the steps for Max-Sum are the same as explained for Max-prod, except the Max-Sum function lacks the utility value on the denominator and is not normalized by utility function [22].

$$MCS^*_{k,n}(m) = argmax_{1 \le MCS_{index} \le 15} \sum_{s=1}^{S_m} u_n^k(m,s) \ . R_{MCS} \quad (4\text{-}7)$$

$$\boldsymbol{k_n}(\boldsymbol{m})^* = argmax_{1\le k\le L}\left\{\sum_{s=1}^{S_m} u_n^k(m,s).{R_{MCS}}^*\right\} \quad (4\text{-}8)$$

$$\boldsymbol{m_n^*} = argmax_{1\le m\le M}\left\{\sum_{s=1}^{S_m} u_n^{k^*}(m,s).{R_{MCS}}^*\right\} \quad (4\text{-}9)$$

4.4 Round Robin-Max_Sum Scheduling Algorithm

The multicast group is selected in round robin fashion, but the transmission rate and video layer are selected by usual Max_Sum algorithm.

$if\ (\ (m_{n-1}^* + 1) \le M)\ then\ m_n^* = m_{n-1}^* + 1$
$else\ m_n^* = 1$

$$MCS_{k,n}^*(m_n^*) = argmax_{1\le MCS_{index}\le 15} \sum_{s=1}^{S_m} u_n^k(m_n^*, s)\ .R_{MCS}$$

$$\boldsymbol{k_n}(m_n^*)^* = argmax_{1\le k\le L}\left\{\sum_{s=1}^{S_m} u_n^k(m_n^*, s).{R_{MCS}}^*\right\}$$

4.5 Multi Groups- Max_Sum Scheduling Algorithm

Initially, the algorithm finds the transmission rate and video layer for each multicast group, according to Max_sum algorithm.

$$MCS_{k,n}^*(grp) = argmax_{1\le MCS_{index}\le 15} \sum_{s=1}^{S_m} u_n^k(grp, s)\ .R_{MCS}$$

$$\boldsymbol{k_n}(grp)^* = argmax_{1\le k\le L}\left\{\sum_{s=1}^{S_m} u_n^k(grp,s).{R_{MCS}}^*\right\}$$

$$Max.sum.value(grp) = \sum_{s=1}^{S_m} u_n^{\boldsymbol{k_n}(grp)^*}(grp,s).{R_{MCS}}^*$$

It also saves the total sum of the user's utility value for the selected layer of each multicast group in an array (Max.sum.value).

Then the algorithm scans through the MSC from lowest to highest value and finds the MSC for which the total sum of the multicast group's utility, "multicast_grp_total_Maxp," is maximized.

For MSC_idx=1:15
S=0;
For grp=1:grp_no

If(MSC_idx< $MCS^*_{k,n}(grp)$)
s=s+ $Max.sum.value$ (1,grp)
End
Total_multigroup_Max_prod(1,MSC_idx)=s;
End
Max_MSC = argmax(Total_multigroup_Max_prod)

Max_MSC is the transmission rate index with more than two supporting groups, and if the aggregated packet is scheduled with that transmission rate, the final sum of all users' utility function in those groups are maximized.

The next step is to find the groups that support the transmission rate (*Max_MSC*)

For grp=1:grp_no
If(Max_MSC <= $MCS^*_{k,n}(grp)$)
Multi_Group_support(1,idx)=grp;
idx=idx+1;
End

Sort the "*Multi_group_support*" from the highest value of their "*Max.sum.value*" to the lowest.

sort(Multi_group_support,'descend')

Now that the lists of groups to be potentially scheduled with *Max_MCS* are available, the next step is to find how many PRB or frequency resources each group needs

For i= 1:Length(Multi_group_support)
NRB(1,i)= Find(NRB for each group according to transmission rate with MSC= Max_MSC and Potential video layer of group)
End

Having the value of required PRB per group lets the scheduler decide how many groups can be scheduled together. The total number of available PRB is 50, so the algorithm picks the group to be scheduled from the first member of array until the sum of PRB reaches the 50.

S=0
For i=1: length(NRB)
If((S+NRB(1,i))<=50)
Group_tobe _Schedule(idx)=Multi_group_support(i)
Layer_tobe_scheduled(idx)= $k_n(i)^*$
idx=idx+1
S=S+NRB(i)
End
End

At this step, the list of groups to be scheduled together is available for scheduler. However, in the final step, the algorithm checks to see if there is more than one group available in the list. If the group list is empty or only has one member, the scheduler drops the list and uses the ordinary Max_Sum method to decide transmission rate, video layer, and multicast group.

4.6 Updating the parameters after scheduling

The average throughput of each layer for every user is updated after scheduling decision in the main loop .

$$r_{k,n}(m,s) = (1-w)r_{k,n-1}(m,s) + R^{*}_{k,n}(m,s).1_{grp=m\,,layer=k}.1_{R^{*}_{k,n}\leq R_n}.1_{\,goup=m}.1_{Layer=\,k} \quad (4\text{-}10)$$

The users in the multicast group that are not scheduled do not benefit from the second term of average throughput value. In the next step, the packet loss rate for all users is updated.

$$p_k(m,s) = 1 - \frac{r_{k,n}(m,s)}{\rho_{k,m}} \quad (4\text{-}11)$$

With a new packet loss rate, the utility value for each Multicast group's subscriber is updated according to (3-12).

In the final step, the achieved utility gain for each layer is calculated.

$$u^{k}_{n}(m,s) = {\partial u(m,s)}/{\partial r_k} = \frac{u(m,s)|_{r=r_k(\mathrm{m,s})} - u(m,s)|_{r=\Delta r + r_k(\mathrm{m,s})}}{\Delta r} \quad (4\text{-}12)$$

It is possible for a user utility to drop to zero. This can be due to deep fading areas, or the users may not be scheduled for a while, resulting in their basic layer packet loss reaching more than 10%. A utility level of zero causes computational errors during Max_prod scheduling, and the user with zero utility fails to help maximize average throughput, therefore that user should be excluded from system decision.

As soon as system faces a user with zero utility value, an assigned counter to that user starts. When the counter value reaches a predefined threshold, the system resets the user's basic layer throughput to the initial value of coding rate and updates its utility value. This method prevents the user from remaining on the outage state forever if the scheduler misses the groups to schedule for a while. Also it gives an opportunity for users to get out of the deep fading area if the user's zero utility is due to low SINR and again have the chance of being scheduled.

5 Simulation Methodology

5.1 General Simulation Procedure

At each TTI, based on the reported SINR of the subscriber, the scheduler decides the multicasting group, video layer, and the modulation and coding rate. Users would be informed of the index of modulation and coding rate scheme before data is multicast. The modulation, coding index, and CQI table are exactly compatible. Despite the transmission scheme, users are aware of scheduled multicast groups and video layer. Upon the completion of decision, the information is passed to the physical layer to form the OFDM symbol. Signal output is tuned to the predefined output power and sent out through the propagation channel.

On the receiver side, the SINR value is calculated. If the user belongs to the scheduled multicast group, it checks if the current SINR is equal to or larger than the required SINR threshold for the transmission scheme. If the SINR is less than the threshold, subscriber drops the packet. A larger SINR permits the packet to be delivered error-free to application layer. The average throughput per layer, packet loss rate, and the other parameters are updated according to Section 4-6.

For each scheduled user, a counter updates with the total received bytes for each layer. The counter shows the exact number of bytes received per layer, and by the end of one second, it reveals the exact rate of packet loss. The quality of service for a user can be checked based on this counter per second. On each second, after the performance calculation is accomplished the counter is rest to zero and performance metrics are measured. If the simulation runs for *10* seconds, the average of metrics value over the past 10 seconds are represented as simulation results.

Each 20ms, the users are moved according to mobility scenario and channel coefficient, and path loss and fading are updated.

5.2 Simulation Scenario

To analyze the behavior of the scheduling algorithm on the MBSFN and single-cell PtM network, different scenarios are implemented in this Master's thesis. In one scenario, video stream type is changed from multilayer to single-layer, and in the other scenario, network topology is changed from MBSFN to Multicast cast within one cell.

5.2.1 Multilayer Streams with Max-Sum, Max-Prod, and RRB-Max_Sum Algorithms on MBSFN Network with Full-rate Transmission

In this scenario, a simulation is run for 6 different cell traffic loads, and in each time, the total number of multicast groups (cell traffic load) increases. The multicast group numbers start from 8 groups (equal to 5.6 Mb/s traffic load) in the first round and ends with 48 (equal to 34 Mb/s cell traffic load). The network topology is MBSFN, and a Multilayer stream is assigned to each multicast group. Some groups may have the same video stream but are independently scheduled. The scheduler transmits with full-rate throughput (PRB=50)

5.2.2 Single layer- Video Streams with Max-Sum and Max-Prod Algorithms on MBSFN Network with Full-rate Transmission

This is the same as scenario one, but the video streams are single-layer.

5.2.3 Multilayer Streams with Max-Prod and Max_Sum Algorithms on Single Cell with Full rate transmission

This is similar to scenario one, but the packets are only multicast within a central cell, and the signals from all neighboring eNodeBs are considered interference.

5.2.4 Multilayer Streams with Max-Sum and Multi group- Max_Sum Algorithm on MBSFN Network with Buffer Model Transmission (Real-time streaming)

This is a test scenario to check the behavior of the system while the buffer model is used, and the scheduler is limited to only transmit bytes of buffer. The simulation parameter and setting are the same as scenario one, but the throughput is not full-rate.

For each scheduling algorithm, an independent test is run, and the results are compared.

5.3 Performance Metric

To evaluate the performance of different algorithms, we use two main metrics: average user utility, which is the average of utility of all subscribers, including those in the outage area, and outage probability, which is the probability of users with utility values equal to zero. There are some other submetrics, like histograms of the distribution of the number of times video layers are scheduled, instantaneous average throughput for arbitrary users, and histograms of the distribution of the CQI value and multicast group number during the simulation.

6 Result and Analysis

6.1 System Capacity on the MBSFN and Single-Cell Mode

System capacity is the average throughput that eNodeB is offered during simulation. The affordable throughput of the system depends on the bandwidth and the user's SINR. The maximum throughput is achieved when all users have high SINR, and scheduler always transmits with highest CQI.

Figures (6-1, 6-2) show the normalized number of times that a CQI value is used in the MBSFN and single-cell-PtM transmission types, respectively. A CQI value corresponds to a transmission rate.

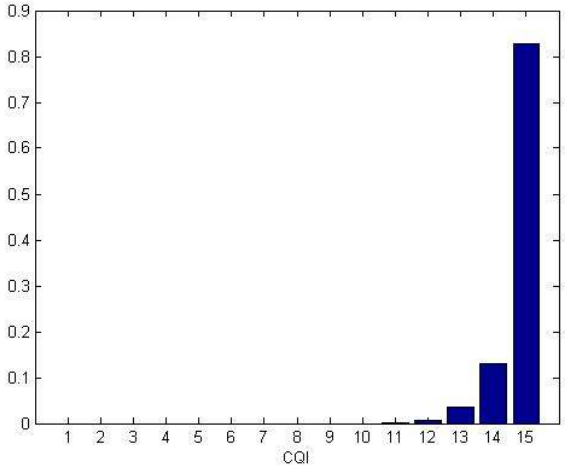

Figure 6-1 : CQI distribution for MBSFN simulation

The average CQI value can be obtained from Figures (6-1, 6-2) and the average system throughput

$$Average\ SC\ system\ throughput = Rate\left(CQI_{avg}\right) * PRB \approx 10\ Mb/s$$

$$Average\ MBSFN\ system\ throughput \approx 29.5\ Mb/s$$

Where the rate for each CQI value can be obtained from Table (3-1) and *PRB=50*.

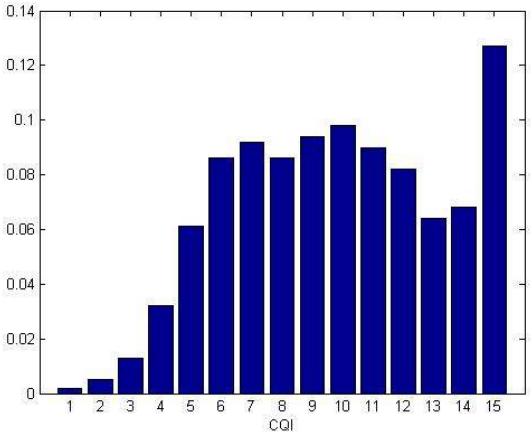

Figure 6-2 : CQI distribution for SC PtM simulation

It should be noted that the average system throughput is shared among the users, but not all users has benefit from that. As the SINR distribution curve shows in Figure (6-3), for SC_PtM transmission type, we always expect at least 5% of users will be in an outage area (in dense user distributions). Due to their low SINR, they can never receive a packet error-free, even if their groups are scheduled in a TTI.

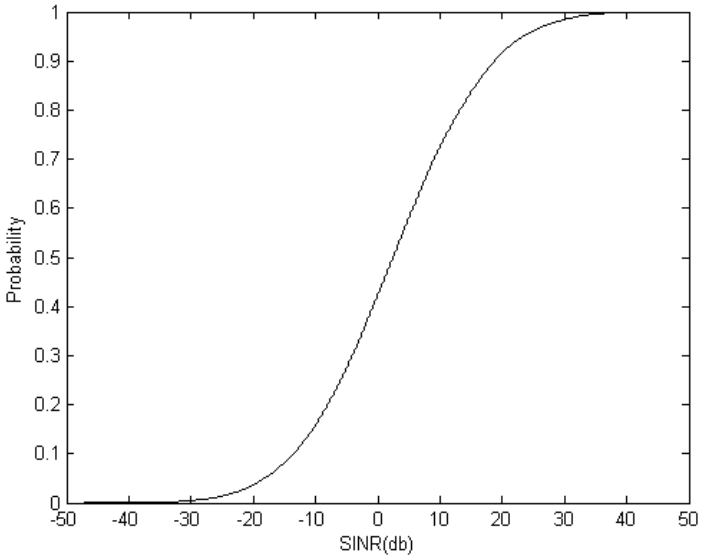

Figure 6-3 : SINR distribution in SC PtM

6.2 Performance of Scheduling Algorithm on SC_PtM Mode

Figures (6-4, 6-5) show the performance of Max_Sum and Max_Prod algorithms in SC_PtM when the scheduler uses full-rate (no buffer Model) to deliver a multilayer stream. As expected, Max_Sum performs better than Max_prod in cases of average utility, because Max_Sum tries to

maximize the throughput regardless of fairness among the groups, which results in higher average utility.

Although Max_Sum results in the higher average utility, it suffers from a bit higher outage probability in comparison to Max_prod. Max_prod offers fairness among the groups and tries to fairly share the system capacity within the groups .while Max_sum always schedules groups that would result in higher total throughput, which is why some groups may be scheduled less frequently. The fairness behavior of Max_prod would result in more groups receive the basic layer packet and at least would be out of outage criteria. The difference between outage probabilities in the Max_Sum and Max_Prod scheduling becomes larger as the multicast group number or cell traffic load increases.

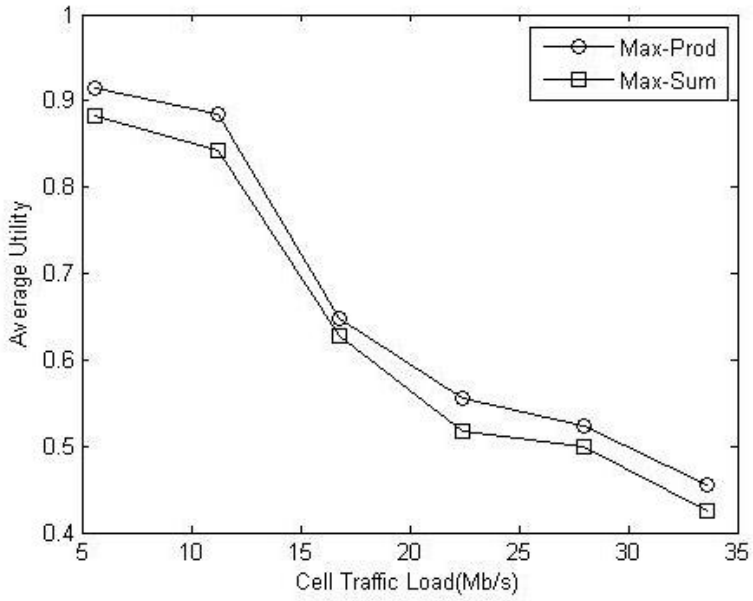

Figure 6-4 : Average Utility of SC PtM-Full-rate- Multilayer Stream Simulation

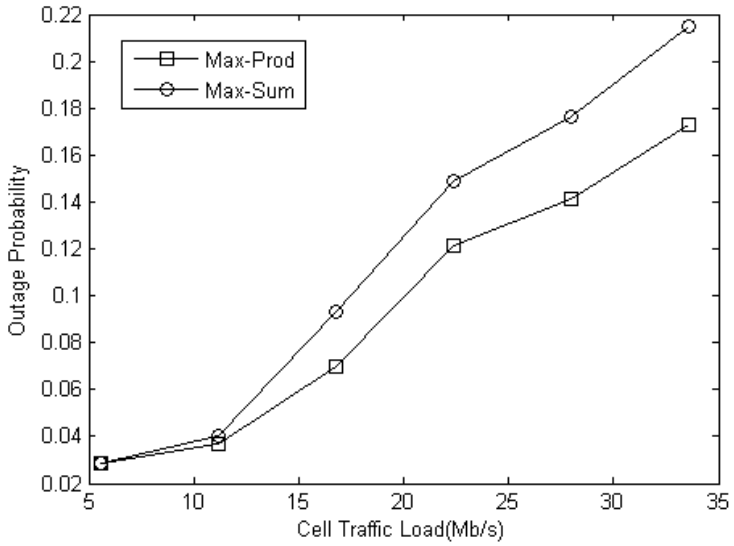

Figure 6-5 : Outage Probability of SC PtM-Full-rate- Multilayer Stream Simulation

6.3 Performance of Scheduling Algorithm on MBSFN Mode

6.3.1 Scheduling Multicast groups with SVC-Stream and full Rate Transmission.

In the contrast to SC_PtM mode, the Max_Prod and Max_Sum algorithms have the same performance when they are supposed to deliver SVC stream to the user on an MBSN network.

Since the users on the MBSN network benefit from high SINR, there is always potential to receive high throughput, and a user in such a group would rarely be in an outage area. Basically, average throughput is big enough on the MBSFN mode that one can think maximizing the throughput ineffective. This can be determined by looking at Figure (6-1), which shows CQI distribution during the simulation. The statistics reveal that most groups are scheduled with the same transmission rate. Therefore, there is no priority among the groups based on the throughput they would receive, but the priority goes to a group for which with the same throughput would result in higher utility.

Because the scheduler always chooses the groups based on the gains that system achieves from utility function, when the average received throughput for all users is rather high, the utility function value approaches one, and the gain for a group with user utility equal to one approaches to zero. Sometimes, when all groups are saturated, the scheduler should choose some groups randomly. In low and average cell traffic loads, the scheduler always tries to share the resources fairly.

Figure (6-6) shows how the scheduler distributed system capacity (29 Mb/s) among the multicast groups when the cell traffic load was 34 Mb/s.

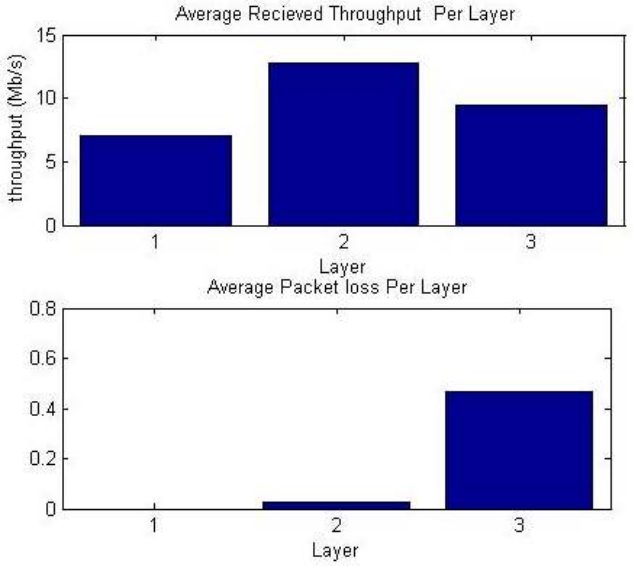

Figure 6-6 : Average received throughput and packet loss rate for cell traffic load = 34 Mb/s

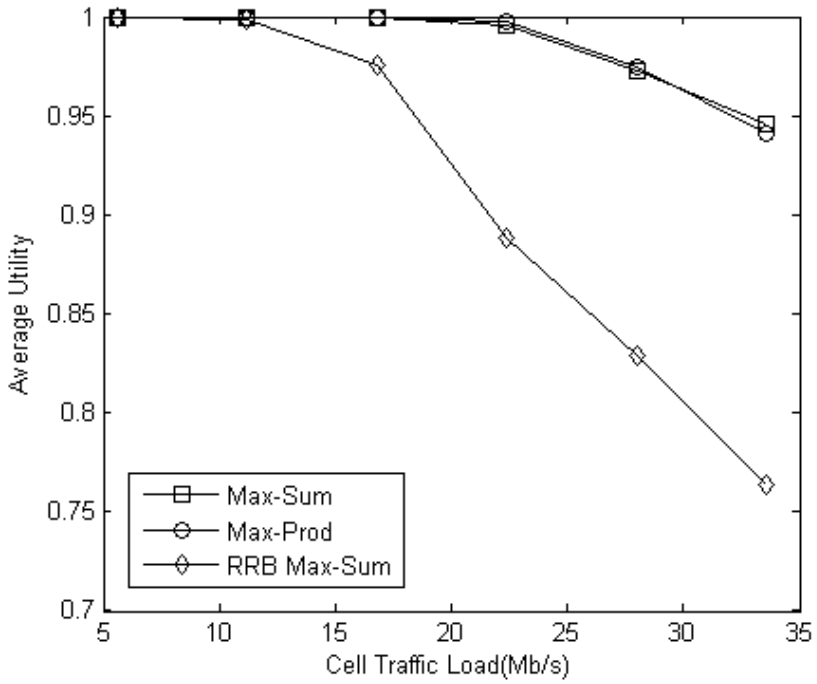

Figure 6-7 : Performance result of full-rate transmission model

The performance of the system falls when the cell traffic load reaches the system capacity (29 Mb/s). Thereafter, the scheduler must drop some enhanced layer packet to fit the available throughput to the system capacity, so the packet loss rate in the third layer increases when cell traffic load enlarges. Dropping some enhanced layers results in lower average utility in high cell

traffic load. However, as Figure (6-6) shows, the total sum of received throughput per layer is still around 29 Mb/s.

One may think if the scheduler distributes the scheduling opportunity fairly among the groups and in each TTI and only decides the video layer of the selected groups, the fairness would be guaranteed, and system performance would improve. But as the simulation results show, this assumption is wrong. In the Round Robin Scheduling, each groups has the same share of scheduling opportunity, and if we assume all the groups are scheduled with approximately the same transmission rate (which is not so far wrong), in the RRB-Max_sum scheduling prototype, all the groups receive equal shares of system capacity. However, the point is that different groups have different video stream properties with different coding rates, so it is obvious that the group with higher video stream coding rate should receive a greater share of system capacity and be given a higher chance of scheduling opportunity.By not only the selecting the video layer, but also by selecting the multicast group for stream packet, the scheduler tries to maximize user utility. It is expected that multicast groups have the different scheduling opportunity rates as Figure (6-8) shows. Figure (6-8) reveal that the multicast groups doesn't have the same share of scheduling opportunity.

With Max-Sum scheduling, average user utility reaches almost 1 in up to 25 Mb/s cell traffic loads. However, with the same conditions (user distribution and cell traffic load), when the system uses Round Robin Multicast group selection, the average user utility drops to around 0.87.

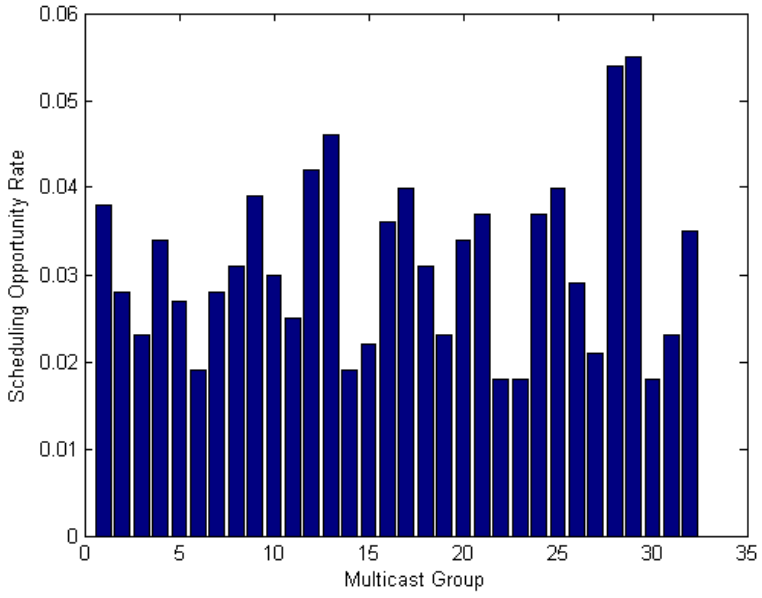

Figure 6-8 : Multicast group selection distribution on MBSFN-Multilayer-Full rate-Max_sum

6.3.2 Scheduling Multicast groups with Single layer -Stream and full Rate Transmission.

It is expected that there would not be any difference by using single-layer and multilayer streams when the system can afford enough throughput to deliver the whole layer's packets. In low and average cell traffic loads, unless the cell traffic does not reach 29 Mb/s, the average user utility is

close to 1 for both Single layer and multilayer stream. But as we have said, when the cell traffic load is beyond the system capacity, the scheduler has to drop some packets. However, the behavior of scheduling algorithms results in different performances.

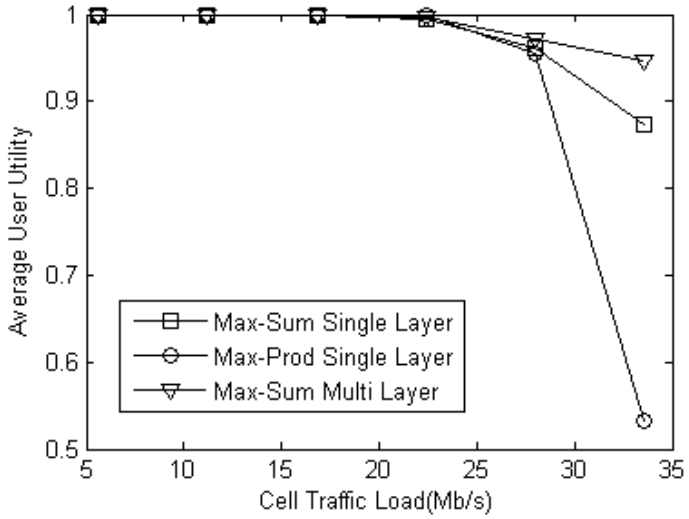

Figure 6-9 : Average utility of MBSFN- Full rate-Single layer Simulation

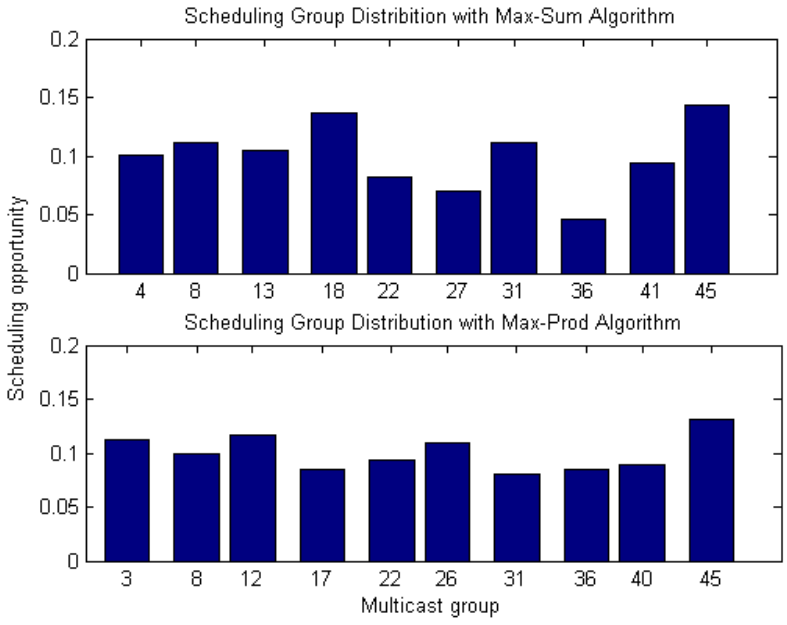

Figure 6-10: Multicast group selection distribution on MBSFN-Single layer-Full rate

As mentioned during introduction to system model, the number of users per multicast group is random, so while a multicast group may have 8 subscribers, the other one may only have 1 user

as member of group. Obviously, the system achieves greater utility gains when a group with more subscribers is scheduled. Keeping same transmission rate for all multicast groups, the randomness of the subscriber numbers of a group and video stream parameters are two factors that affect the utility gain.

One can say Max-Sum always gives priority to the groups with bigger subscribers (ignoring the effect of stream type), while Max-Prod tries to keep fairness of scheduling opportunity among the Multicast groups. This can be inferred from Figure (6-10). There are some groups in the Max-Sum Scheduling simulation result that have higher shares of scheduling opportunities, while the other groups may have few shares. The fairness behavior of Max-prod is not as precise as Round Robin, but with small variation, it is generous to accept the fairness behavior of Max-prod Algorithm in the distribution of scheduling opportunity for single-layer multicasting. Although this fairness behavior results in lower outage probability when the system approaches its capacity, when it comes to high cell traffic loads, the fairness is no longer useful, and it causes higher packet loss rate among all groups, and outage probability increases sharply.

Figure 6-11 illustrated the outage probability of single layer and multilayer streaming in MBSFN. Unless the packet loss rate of the basic layer of the multilayer stream is less than 10%, there is no outage. This goal is always achievable, even in high cell traffic loads in MBSFN, but in the case of single-layer, a packet loss of 10% causes the whole received video packet to be impossible to decode, and user would be considered in the outage criteria. The system is sensitive to the packet loss rate in the single-layer streaming, and due to the higher coding rate of a single-layer stream, particularly after the cell traffic load crosses the system capacity, outage probability becomes much bigger than in the multilayer case.

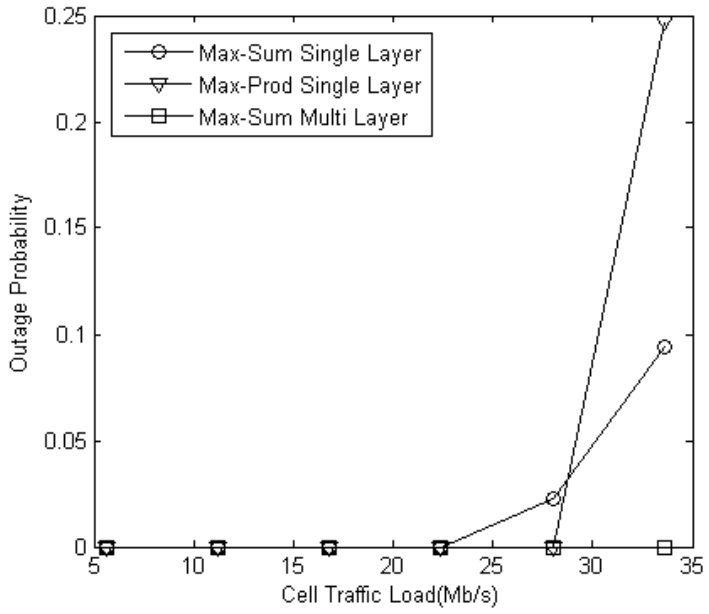

Figure 6-11 : Outage probability of MBSFN-Single layer and Multilayer-Full rate

6.4 Scheduling Multicast Groups with SVC-Stream Using Buffer Model

In the proposed buffer model, the streaming is real–time, and the users of scheduled groups only receive the packets that are stored in the limited-length buffer from previous scheduling time.

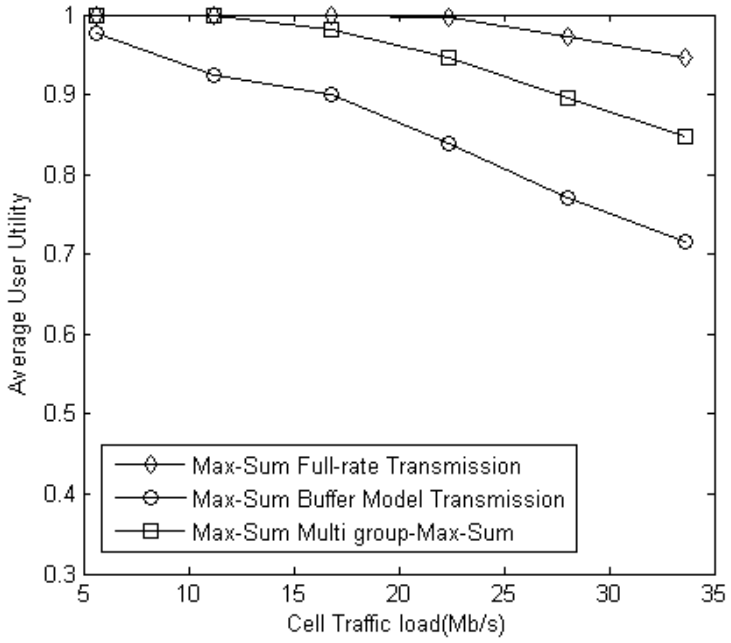

Figure 6-12 : Average utility of MBSFN- Buffer Model Transmission-Multi layer simulation

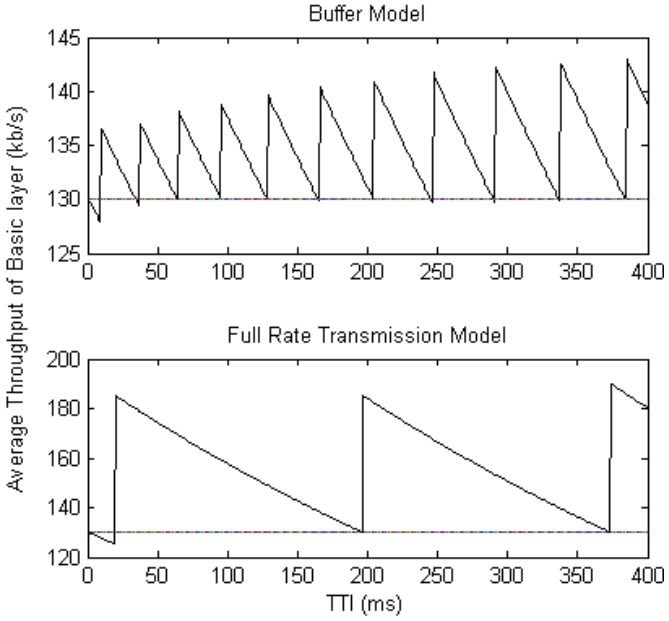

Figure 6-13 : Average Throughput for Basic layer of an arbitrary user (Cell traffic load= 23 Mb/s)-MBSFN-Multilayer

As Figure (6-12) shows, although the user distribution and video stream allocation to each multicast group and cell traffic load are the same with the full-rate transmission scenario, there is still a big performance gap between the two scenarios, and the buffer model has a much lower average user utility. The reason can be found through Figures (6-13, 6-14).

The average widowing factor, *w*, should be low enough to keep the average throughput around the coding rate. Thus, average throughput toward a data burst is reluctant, meaning only a large enough data burst can significantly change the average throughput. The data burst size or instantaneous throughput of full-rate transmission is so high that, with one time scheduling, the average throughput of the basic layer increases significantly, and the layer would be saturated for a long time. When the basic layer is saturated, it lets the scheduler deliver an enhanced layer to the multicast group. As Figure (6-13) shows ,the time duration that the basic layer stays saturated after receiving the data packet bursts is long in full-rate therefore It is more feasible to have another enhanced layer scheduled. This can be found from Figure 6-14, that the opportunity of enhanced layer scheduling is much higher than buffer model. On the other hand, due to small data bursts on the buffer model transmission, the average throughput is not as high after each scheduling opportunity, and the amount of time that the basic layer would stay saturated is low. This would force the scheduler to give priority to basic layer to prevent packet loss rate from falling beyond the 10%.

Small data bursts in the buffer model would result in average throughput with small variations around the coding rate. Since the enhanced layers are not scheduled as much in the buffer model, average utility is lower than in full-rate.

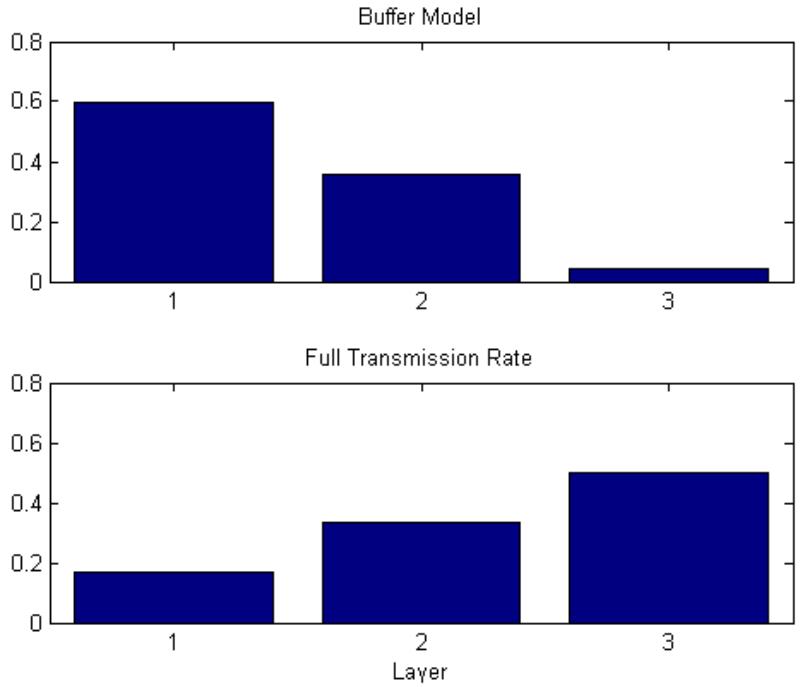

Figure 6-14: Distribution of Layer selection in full and buffer model transmission -MBSFN -Max_Sum

Aggregating small data bursts in a larger packet and scheduling two or more groups at the same time would result in much better average user utility, and the system would approach its ideal performance (full-rate transmission). The advantage of multigroup scheduling is that the scheduler can efficiently use the time duration that base layer is saturated and schedule more enhanced layers of other groups.

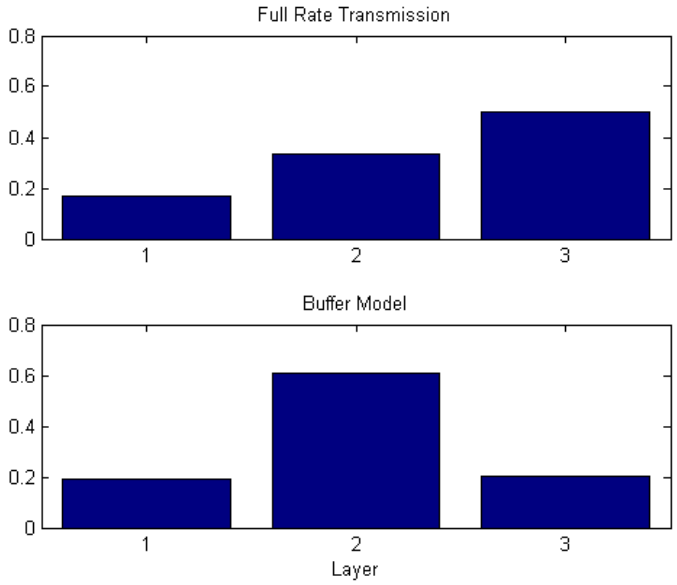

Figure 6-15 : Distribution of Layer selection MBSFN- full rate- Max-Sum and Multi group –Max_Sum Scheduling

It has been mentioned that the buffer is limited in length. For the low cell traffic load, it may not seem important to have a large buffer, but as the cell traffic load increases, the time interval between two consecutive occasions that a layer of group is scheduled increases. Thus, there would be a demand to have higher buffer capacity.

Figure (6-16) shows the distribution of time intervals between two occasions for which a layer of the group is scheduled when the cell traffic load is 17 Mb/s. As displayed , most delays are less than 200ms.

Figure (6-17) shows the effect of buffer length on the average user utility when cell traffic load is 17 Mb/s. When buffer length is beyond the 200ms, there would be no significant increase in average user utility, so one can think a buffer with 200ms can act as infinite buffer length.

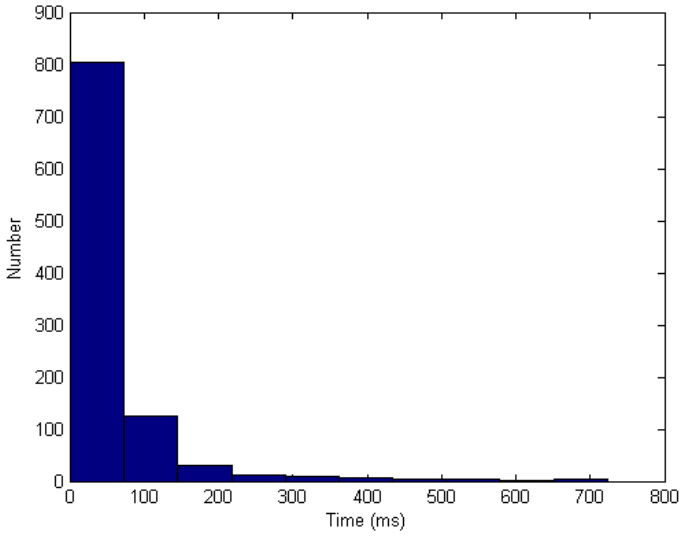

Figure 6-16 : Distribution of the delay between two occasions of same layer scheduling (Cell traffic load =17 Mb/s)-MBSFN-Multilayer stream

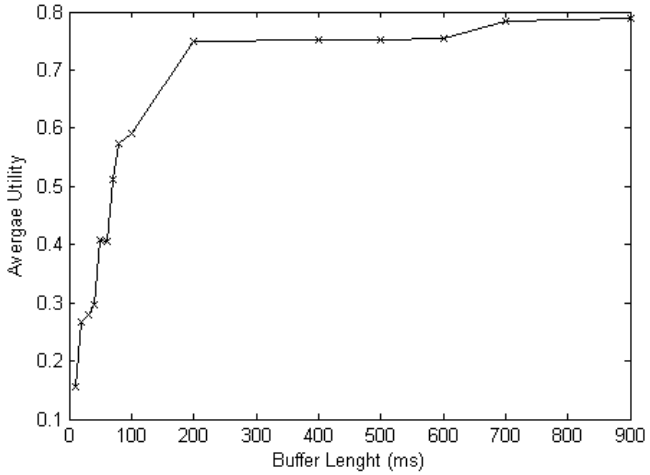

Figure 6-17 : effect of Buffer length on Average user distribution

7 Conclusion

This Master's thesis presents a multicasting technique and three scheduling algorithms to deliver Multimedia stream to end-user over a single frequency network (SFN).

The macro-diversity feature of MBSFN results in the received copy of the signal with a delay smaller than cyclic prefix would add constructively. Therefore, the user has a much higher SINR compared to single-cell PtM transmission. A high SINR value gives the user potential to receive high transmission rate which would result in better user utility.

Four multicast scheduling algorithms -Max_Sum, Max_Prod, Round Robin-Max_Sum, and Multi Group-Max_Sum—are implemented in different scenarios. Regardless of video type, Max_Sum scheduler chose the multicast group and a video layer for scheduling in a way that maximized the system utility gains. On the other hand, Max_Prod tries to keep fairness on distribution of system resources.

It has been shown that, no matter what type of video stream is used (single-layer, multilayer) and regardless of the scheduling algorithm (Max_Prod, Max_Sum), the MBSFN techniques perform much better in comparison to SC PtM. In single-cell, multicasting a multilayer stream with the Max_Sum scheduler would result in higher average user utility and overall quality of service compared to using the Max_Prod algorithm is better, but with price of higher outage probability.

We have shown that the performance of multicasting a multilayer stream over MBSFN with Max_prod and Max_sum Scheduler would result in the same performance and average user utility if the scheduler allocated full resources (full-rate transmission). Although RRB -Max_Sum guarantees the fairness of sharing the resources among the multicast groups, it has a lower performance. This is because different Multicast groups have different subscriber numbers and video coding rates, so they should not necessarily require to receive the same share of system capacity.

Multicasting single- and multilayer streams may have the same performance on average and low cell traffic loads, but as the cell traffic load crosses the system capacity, due to a higher packet loss rate. multilayer streaming would perform better because it loses the packets on the enhanced layer, and the system can still afford the basic layer packet delivery. Single-layer streams are not resilient against the packet loss, so the average utility drops when packet loss rate starts to appear. Multicasting a single-layer video stream with Max_Sum would result in better picture quality and lower outage probability in higher cell traffic loads.

We have presented the effect of the buffer model. The demand of the buffer model appears when the streams are real-time and the scheduler is limited to transmitting only the data that are stored on the buffer and some resources remained unused. This is the opposite of full-rate transmission that lets the scheduler access the data as much as the frame size permits.

Since the data burst with buffer model is small, the average received throughput on the basic layer would not change significantly by each scheduling occasion, and the basic layer stays saturated for a shorter time. This forces the scheduler to have a lower chance of scheduling the other enhanced layer. Since the subscriber receives fewer enhanced layer packets, the average utility is lower than full-rate transmission. To overcome this problem, the Multigroup–Max_Sum scheduler is presented. By aggregating the small data burst of some multicast groups, it uses the system resources efficiently. Since two or more multicast groups are scheduled at the same time, the scheduler would have more chance to transmit the enhanced layer packet while the basic layer is saturated and have less than a 10% packet loss rate.

In the simulation result, we have shown that buffer lengths bigger than the specific threshold does not significantly increase the average user utility, but with less than specific level, the average user utility is degraded.

8 Future Work

The mobility scenario is a bit elementary on the system model, and it is only limited to the central cell. The disadvantage of this issue is that it was not possible to check the effect of speed and mobility on the performance of different algorithms and scenarios. The subscriber is only a pedestrian who walks slowly with random motion. In the real world, there are users with high speeds while on trains, buses, or cars. There is no obstruction model in the physical layer simulation and system model. This would mean that no user would enter a deep fading area, which is entirely possible in the real situation. Adding a better mobility simulation scenario with obstruction model and correlated shadow fading distribution would be a big step for future work.

Although cyclic prefix compensates the delay of path, to cover large area, it is not possible to have only one SFN network, due to a larger delay of received signals. It is common to have two or more SFN networks which are geographically located over service area. One can go into the details of resource allocation on each SFN in such a way to decrease the interference of other networks.

There can be some modification of the physical layer model. The wireless system model is a basic hexagonal site with Omni antenna on the middle. However, most mobile networks have a directional antenna with 3 sectors per site. This may affect the SINR value, but not the algorithm logic. Moreover, one of the key features of LTE technology is the use of MIMO, which results in the better received throughput, and therefore better performance and quality of service for multicast streaming.

The frequency domain scheduling algorithm is not covered in this master thesis. It would be an interesting area of research to combine time domain and frequency domain together. While in time domain the multicast groups are fighting for scheduling opportunity, on the frequency domain they are competing for the PRB that have best CQI on that , Therefore the UE doesn't report a wideband CQI but only report the CQI for the allocated PRB. The formula of SINR is changed and it is limited to the allocated PRB. The SINR mapping table still would be the same Table 3-1 , but the formula 3-2 should be used to tune the calculated SINR to effective SINR.

References

[1]. E. Biglieri. "*Coding for Wireless Channels*". Springer, 2005.

[2]. Yu Shuan Yeh Larry J. Greenstein, Vinko Erceg and Martin V. Clark. "*A new path-gain/delay-spread propagation model for digital cellular channels*", IEEE Transactions on Vehicular Technology, VOL.46, MAY 1997.

[3]. Heidi Himmanen ,"*Studies on channel models and channel characteristics for mobile Broadcasting* ". Broadband Multimedia Systems and Broadcasting, 2008 IEEE International Symposium ,April 2 2008

[4] M. Hata. "*Empirical formula for propagation loss in land mobile radio services*". IEEE Transactions on Vehicular Technology, 29, 1980.

[5] J.Walfisch and H.L. Bertoni. "*A theoretical model of uhf propagation in urban Environments*". IEEE Trans. Antennas Propagat., 36, 1988.

[6] T.B. Sorensen. "*Correlation model for slow fading in a small urban macro cell. In Personal, Indoor and Mobile Radio Communications, 1998*". The Ninth IEEE International Symposium on, volume 3, pages 1161–1165 vol.3, Sep 1998.

[7] L. Vuokko J. Salo and P. Vainikainen. "*Why is shadow fading lognormal*". Proc. International Symposium on Wireless Personal Multimedia Communications Aalborg, Denmark, pages 522–526, 2005.

[8] V. Graziano. "*Propagation correlations at 900 mhz"*. IEEE Transactions on Vehicular Technology, VT-27, 1978.

[9] T. Keller and L. Hanzo, "*Adaptive modulation techniques for duplex OFDM transmission*", IEEE Transactions on Vehicular Technology, vol.49, no.5, pp.1893-1905, Sept. 2000.

[10] Cimini, L., Jr. , "A*nalysis and Simulation of a Digital Mobile Channel Using Orthogonal Frequency Division Multiplexing* ",Transactions on IEEE Communications, Volume: 33 , Issue: 7 ,1985

[11] Koffman, I.; Roman, V ,"*Broadband wireless access solutions based on OFDM access in IEEE 802.16"*,Communications Magazine, IEEE Volume: 40 , Issue: 4 - 2002 , Page(s): 96 - 103

[12] Rong, L. Elayoubi, S.E. "*Analytical Analysis of the Coverage of a MBSFN OFDMA Network*",Global Telecommunications Conference, New Orleans , Dec-2008.

[13] R. Rebhan and J. Zander *"On the Outage Probability in Single Frequency Networks for Digital Broadcasting"*, IEEE Transaction on Broadcasting, Vol. 39, No. 4, pp. 395, December 1993.

[14] R. Brugger and D. Hemingway *"OFDM Receivers - Impact on Coverage of Inter-symbol Interference and FFT Window Positioning"*, EBU Technical Review, July 2003.

[15] 3GPP TR 25.942, *"*Technical Specification Group Radio Access Networks RF System Scenarios*"*, V5.1.0, 1999.

[16] Sushruth N. Donthi and Neelesh B. Mehta , "*Performance Analysis of Subband-Level Channel Quality Indicator Feedback Scheme of LTE* ".National conference of Communications (NCC) – march 2010 ,

[17] R.Sandanalakshmi,"*Effective SNT Mapping for link error prediction OFDM based systems*". IET-UK International Conference on Information and Communication Technology in Electrical Sciences (ICTES 2007),
Dr. MG.R. University, Chennai, Tamil Nadu, India. Dec. 20-22, 2007. 684-687.

[18] Josep Colom Ikuno, Martin Wrulich, Markus Rupp ,"*System level simulation of LTE networks*",2010 IEEE 71s Vehicular Technology Conference : VT2010-Spring .

[19] H. Steendam and M. Moeneclaey. "*Analysis and optimization of the performance of OFDM on frequency-selective time-selective fading channels*". Transactions on IEEE Communications ,47(12):1811–1819, Dec 1999.

[20] Pei Chang, Yongyu Chang, Yunan Han, Chi Zhang, Dacheng Yang,"*Interference Analysis and Performance Evaluation for LTE TDD System*". In Proc. of Advanced Computer Control (ICACC), 2010 , Page(s): 410 - 414

[21] 3GPP TR 25.892 Feasibility Study for Orthogonal Frequency Division Multiplexing (OFDM) for UTRAN enhancement.

[22] Vladimir Vukadinović ,György Dán "*Multicast Scheduling for Scalable Video Streaming in Wireless Networks*". ACM Multimedia Systems (MMSys), Scottsdale, AZ, Feb. 2010.

[23] Heiko Schwarz, Detlev Marpe, and Thomas Wiegand ,"*Over view of Scalable video Conding H.264/MPEG4-AVC extension*". Image Processing, 2006 IEEE International .page 161 - 164

[24] SVC Reference Software. [Online]. Available: http://ip.hhi.de/imagecom_G1/savce/downloads/SVC-Reference-Software.htm

[Accessed oct.2010].

[25] P. Bender, P. Black, M. Grob, R. Padovani, N.Sindhushayana, and A. Viterbi, "*CDMA/HDR: A bandwidth efficient high speed wireless data service for nomadic users*," IEEE Commun. Magazine, vol. 38, pp. 70–78, July 2000.

[26] O. Verscheure, P. Frossard, and M. Hamdi, "*User-oriented QoS analysis in MPEG-2 video delivery*," Journal of Real-Time Imaging, vol. 5, no. 5, pp. 305–314, Oct. 1999.

[27] .Harri Holma and Antti Toskala "*LTE for UMTS: OFDMA and SC-FDMA Based Radio Access* "2009 John Wiley & Sons, Ltd. ISBN: 978-0-470-99401-6.

[28] 3GPP TS 36.300: "Evolved Universal Terrestrial Radio Access (E-UTRA) and Evolved Universal Terrestrial Radio Access (E-UTRAN); overall description; Stage 2".

[29] 3GPP TS 36.331 "Radio Resource Control (RRC);Protocol specification"

[30] 3GPP TS 23.246: "Multimedia Broadcast/Multicast Service (MBMS); Architecture and functional description".

[31] 3GPP TS 23.402, 'Architecture enhancements for non-3GPP accesses (Release 8)'.

[32] 3GPP Technical Report, TR 25.913, 'Requirements for Evolved UTRA (E-UTRA) and Evolved UTRAN"

[33] 3GPP TS 23.203 "Policy and charging control architecture"(Release 8)

[34] 3GPP TS 33.401, 'Security Architecture (Release 8)'.

[35] 3GPP TS 33.323 "Packet Data Convergence Protocol (PDCP) specification"

[36] 3GPP LTE Channels and MAC Layer, www.EventHelix.com.

[37] 3GPP TS 33.322 "Radio Link Control (RLC) protocol specification".

[38] 3GPP TS 33.321 "Medium Access Control (MAC) protocol specification".

[39] 3GPP TS 36.413 "S1 Application Protocol (S1AP) specification".

[40] 3GPP TS 29.274 "Evolved GPRS Tunnelling Protocol for EPS (GTPv2)"

[41] 3GPP TS 36.440" General aspects and principles for interfaces supporting Multimedia

Broadcast Multicast Service (MBMS) within E-UTRAN".

[42] 3GPP TS 24.440 “Multimedia Broadcast/Multicast Service (MBMS); Architecture and functional description”

[43] Alexiou, A. Bouras, C. Kokkinos, V. Papazois, A. Tsichritzis, “*Efficient MCS selection for MBSFN transmissions over LTE networks*” ,G. Wireless Days (WD), 2010 IFIP ,Oct. 2010.

[44] Oyman, O.; Foerster, J.; Yong-joo Tcha; Seong-Lee;
“*Toward enhanced mobile video services over WiMAX and LTE*”, Communications Magazine, vol. 48, Issue: 8, 2010.

[45] Alexiou, A. Bouras, C. Kokkinos, V. Tsichritzis, G., “*Communication cost analysis of MBSFN in LTE*” ,Personal Indoor and Mobile Radio Communications ,Sep.2010 .

[46] 3GPP TS 25.346 V8.3.0 Technical Specification Group Radio Access Network; Introduction of the Multimedia Broadcast Multicast Service.(MBMS) in the Radio Access Network (RAN); Stage 2 (Release 8).

[47] 3GPP, TS 22.146 V9.0.0. Technical Specification Group Services and System Aspects; Multimedia Broadcast/Multicast Service; Stage 1 (Release 9).

[48] 3GPP TS 36.300 V9.1.0. Technical Specification Group Radio Access Network; Evolved Universal Terrestrial Radio Access (E-UTRA) and Evolved Universal Terrestrial Radio Access Network (E-UTRAN); Overall description; Stage 2 (Release 9), 2009.

[49] Rong, L. Elayoubi, S.E.” *Comparison of mobile TV deployment strategies in 3G LTE networks*”, Wireless Telecommunications Symposium,. June 2009.

[50] Pei Chang, Yongyu Chang, Yunan Han, Chi Zhang, Dacheng Yang,”*Interference Analysis and Performance Evaluation for LTE TDD System*”. In Proc. of Advanced Computer Control (ICACC) ,March 2010.

[51] Hyungsuk Won Han Cai Do Young Eun Guo, K. Netravali, A. Injong Rhee Sabnani, K. *"Multicast Scheduling in Cellular Data Networks*”, In Proc. Of Computer Communications ,INFOCOM 2007.May 2007.

[52] Schierl, T. Stockhammer, T. Wiegand, T. ,"*Mobile Video Transmission Using Scalable Video Coding*",IEEE Transaction on Circuits and Systems For Video Technology , vol. 17, No. 9, Sep.2007.

[53] P. Bender, P. Black, M. Grob, R. Padovani, N.Sindhushayana,A. Viterbi, “*CDMA/HDR: A bandwidth efficient high speed wireless data service for users*, ”IEEE Commun. Magazine, vol. 38, July 2000.

[54] Heiko Schwarz, Detlev Marpe , Thomas Wiegand ,*"Overview of the Scalable Video Coding Extension of the H.264/AVC Standard"*. IEEE TRANSACTIONS ON CIRCUITS AND SYSTEMS FOR VIDEO TECHNOLOGY, VOL. 17, NO. 9, SEPTEMBER 2007 1103

[55] Shan Lu Yi Cai Li Zhang Jike Li Skov, P. Chunye Wang Zhiqiang He , "*Channel-Aware Frequency Domain Packet Scheduling for MBMS in LTE*" , in proc of. Vehicular Technology,IEEE 69th . April 2009.

[56] Mongha, G. Pedersen, K.I. Kovacs, I.Z. Mogensen, P.E. ," *QoS Oriented Time and Frequency Domain Packet Schedulers for The UTRAN Long Term Evolution*". In Proc. Of Vehicular Technology, VTC Spring 2008. IEEE .

[57] Aoxue Jiang Chunyan Feng Tiankui Zhang ," *Research on resource allocation in multi-cell MBMS Single Frequency Networks"*, In proc. Of Wireless And Optical Communications Networks (WOCN) Sept. 2010 .

[58] Munaretto, D. Jurca, D. Widmer, J. *"Broadcast video streaming in cellular networks: An adaptation framework for channel, video and AL-FEC rates allocation",*In Proc. Of Wireless Internet (WICON), 2010 .

[59] Christian Mehlf uhrer, Martin Wrulich, Josep Colom Ikuno, Dagmar Bosanska, Markus Rupp ,"*Simulating The long term evolution physical layer*", In proc. Of 17th European Signal Processing Conference(EUSIPCO),2009.

[60] Thomas Schierl,Thomas Stockhammer,Thomas Wiegand," *Mobile Video Transmission Using Scalable Video Coding*" ,Transaction on circuits and system for video technology , Vol 17, No.9 September 2007